

Chulalongkorn University

## Chula Digital Collections

---

Chulalongkorn University Theses and Dissertations (Chula ETD)

---

2023

# Effect of type and concentration of acid on characteristics of functionalized biochar and its performance in converting fructose to 5-HMF

Pimlapas Bunwichian  
*Faculty of Engineering*

Follow this and additional works at: <https://digital.car.chula.ac.th/chulaetd>



Part of the [Chemical Engineering Commons](#)

---

### Recommended Citation

Bunwichian, Pimlapas, "Effect of type and concentration of acid on characteristics of functionalized biochar and its performance in converting fructose to 5-HMF" (2023). *Chulalongkorn University Theses and Dissertations (Chula ETD)*. 10213.

<https://digital.car.chula.ac.th/chulaetd/10213>

This Thesis is brought to you for free and open access by Chula Digital Collections. It has been accepted for inclusion in Chulalongkorn University Theses and Dissertations (Chula ETD) by an authorized administrator of Chula Digital Collections. For more information, please contact [ChulaDC@car.chula.ac.th](mailto:ChulaDC@car.chula.ac.th).

Effect of type and concentration of acid on characteristics of  
functionalized biochar and its performance in  
converting fructose to 5-HMF

Miss Pimlapas Bunwichian



A Thesis Submitted in Partial Fulfillment of the Requirements  
for the Degree of Master of Engineering in Chemical Engineering  
Department of Chemical Engineering  
Faculty Of Engineering  
Chulalongkorn University  
Academic Year 2023

อิทธิพลของชนิดและความเข้มข้นของกรดต่อสมบัติของฟังก์ชันนอลไลซ์ไบโอโอสาร์และสมรรถนะ  
ในการเปลี่ยนฟรุกโตสเป็นไฮดรอกซีเมทิลเฟอร์ฟูรัล



วิทยานิพนธ์นี้เป็นส่วนหนึ่งของการศึกษาตามหลักสูตรปริญญาวิศวกรรมศาสตรมหาบัณฑิต  
สาขาวิชาวิศวกรรมเคมี ภาควิชาวิศวกรรมเคมี  
คณะวิศวกรรมศาสตร์ จุฬาลงกรณ์มหาวิทยาลัย  
ปีการศึกษา 2566

Thesis Title                      Effect of type and concentration of acid  
                                                 on characteristics of functionalized  
                                                 biochar and its performance in  
                                                 converting fructose to 5-HMF  
By                                              Miss Pimlapas Bunwichian  
Field of Study                      Chemical Engineering  
Thesis Advisor                      Professor Dr. TAWATCHAI  
                                                 CHARINPANITKUL

---

Accepted by the FACULTY OF ENGINEERING,  
Chulalongkorn University in Partial Fulfillment of the  
Requirement for the Master of Engineering

..... Dean of the FACULTY OF  
ENGINEERING  
(Professor Dr. SUPOT  
TEACHAVORASINSKUN)

#### THESIS COMMITTEE

..... Chairman  
(Assistant Professor Dr. Palang  
Bumroongsakulsawat)  
..... Thesis Advisor  
(Professor Dr. TAWATCHAI  
CHARINPANITKUL)  
..... Examiner  
(Assistant Professor Dr. CHALIDA  
KLAYSOM)  
..... External Examiner  
(Dr. Sanchai Kuboon)

พิมพ์ลภัส บุญวิเชียร : อิทธิพลของชนิดและความเข้มข้นของกรดต่อสมบัติของฟังก์ชันนอลไลซ์ไบโอชาร์และสมรรถนะในการเปลี่ยนฟรุกโตสเป็นไฮดรอกซีเมทิลเฟอร์ฟูรัล. ( Effect of type and concentration of acid on characteristics of functionalized biochar and its performance in converting fructose to 5-HMF) อ.ที่ปรึกษาหลัก : ศ. ดร.รัชชัย ชรินพานิชกุล

ชีวมวลเป็นหนึ่งในพลังงานทางเลือกใหม่ที่ประกอบด้วยสารสำคัญอย่างเซลลูโลส เซลลูโลสสามารถนำไปผลิตเคมีแพลตฟอร์ม ได้แก่ ไฮดรอกซีเมทิลเฟอร์ฟูรัล, ลิวูลินิก, ฟอร์มิกและเฟอร์ฟูรัล ในหลายปีที่ผ่านมา การผลิตไฮดรอกซีเมทิลเฟอร์ฟูรัลจากฟรุกโตสสามารถผลิตได้จากการใช้ตัวเร่งปฏิกิริยาแบบเบกคิงสัน (ตัวเร่งปฏิกิริยาและสารที่ทำปฏิกิริยาอยู่ในสถานะของเหลว) โดยตัวเร่งปฏิกิริยาชนิดนี้สามารถให้ผลผลิตกึ่งขั้นที่ค่อนข้างสูงแต่ก่อให้เกิดการกัดกร่อนอุปกรณ์และยากต่อการแยกผลิตภัณฑ์และสารตั้งต้น ในงานวิจัยนี้จึงทำการพัฒนาสังเคราะห์ตัวเร่งปฏิกิริยาแบบวิวิธกัณฑ์ (ตัวเร่งปฏิกิริยาสถานะของแข็งสารที่ทำปฏิกิริยาสถานะของเหลว) คือ ฟังก์ชันนอลไลซ์ไบโอชาร์จากเปลือกแดงโม ด้วยวิธีการไพโรไลซิสและไฮโดรเทอร์มอล มีขั้นตอนสังเคราะห์ฟังก์ชันนอลไลซ์ไบโอชาร์โดย นำเปลือกแดงโมมาทำการไพโรไลซิสเพื่อสังเคราะห์ ไบโอชาร์เปลือกแดงโม หลังจากนั้นทำการปรับเปลี่ยนพื้นที่ผิวไบโอชาร์เปลือกแดงโมด้วยกรด ด้วยวิธีไฮโดรเทอร์มอล มีตัวแปรที่ศึกษาคือ ชนิดของกรด (กรดไฮโดรคลอริก, กรดซัลฟิวริก, และกรดฟอสฟอริก) และความเข้มข้นของกรด (1.6, 3.2, และ 4.8 นอร์แมลลิตี) การวิเคราะห์คุณลักษณะของฟังก์ชันนอลไลซ์ไบโอชาร์ ทำโดยการใช้กล้องจุลทรรศน์อิเล็กตรอนแบบส่องกราดที่มีสมรรถนะสูง ชนิดฟิลด์อิมิตชัน, เครื่องมือวัดพื้นผิวและรูพรุน, เครื่องวิเคราะห์ธาตุ, เครื่องฟูรีเยร์ทรานฟอร์มอินฟราเรดสเปกโตรมิเตอร์และเครื่องวิเคราะห์ค่าความเป็นกรดด้วยเทคนิคโปรแกรมอุณหภูมิแอมโมเนีย การทดลองประสิทธิภาพของฟังก์ชันนอลไลซ์ไบโอชาร์ทำโดย นำไบโอชาร์ 0.2 กรัมผสมเข้ากับสารตั้งต้นฟรุกโตสที่มีความเข้มข้นร้อยละ 40 โดยมวลต่อปริมาตร ในสารละลายน้ำกลั่น 30 มิลลิลิตร ทำปฏิกิริยาที่อุณหภูมิ 160 องศาเซลเซียส เป็นเวลา 90 นาที จากผลการทดลองพบว่า ฟังก์ชันนอลไลซ์ไบโอชาร์ที่ทำการปรับพื้นที่ผิวด้วยกรดซัลฟิวริก ที่ความเข้มข้น 4.8 นอร์แมลลิตี มีสมบัติทางกายภาพ คือ มีรูพรุนชนิดไมโครพอร์และเมโซพอร์ พื้นที่ผิว 464 ตารางเมตรต่อกรัมและปริมาตรรูพรุน 0.33 ลูกบาศก์เซนติเมตรต่อกรัม พร้อมทั้งมีสมบัติทางเคมีคือ มีหมู่ฟังก์ชันกรด คือ ซันโพนิก ที่สามารถจ่ายโปรตรอนไปยังฟรุกโตส ทำให้เร่งปฏิกิริยาในการเกิดเป็นไฮดรอกซีเมทิลเฟอร์ฟูรัล ซึ่งตัวอย่างมีค่าความเป็นกรดบนพื้นที่ผิว เท่ากับ 4.31 มิลลิโมลต่อกรัม จากการทดสอบประสิทธิภาพในการใช้เป็นตัวเร่งปฏิกิริยา พบว่าประสบความสำเร็จในการเปลี่ยนฟรุกโตสเป็นไฮดรอกซีเมทิลเฟอร์ฟูรัล มีร้อยละอัตราการเปลี่ยนสารตั้งต้นฟรุกโตสเท่ากับ 72, ร้อยละการผลิตไฮดรอกซีเมทิลเฟอร์ฟูรัลสูงสุดเท่ากับ 46, และร้อยละการเลือกเกิดไฮดรอกซีเมทิลเฟอร์ฟูรัลสูงสุดเท่ากับ 63

สาขาวิชา            วิศวกรรมเคมี  
ปีการศึกษา        2566

ลายมือชื่อนิสิต .....  
ลายมือชื่อ อ.ที่ปรึกษาหลัก .....

# # 6470393721 : MAJOR CHEMICAL ENGINEERING

KEYWOR

D:

Pimlapas Bunwichian : Effect of type and concentration of acid on characteristics of functionalized biochar and its performance in converting fructose to 5-HMF. Advisor: Prof. Dr. TAWATCHAI CHARINPANITKUL

Biomass, with its high cellulosic content, represented renewable source capable of being converted into essential platform chemicals like 5-hydroxymethylfurfural, levulinic acid, formic acid, and furfural. Currently, conversion of fructose to 5-HMF was achievable through various acid homogeneous catalysts. Although these catalysts yield higher outputs, they might pose challenges in recycling and corrosion issues. This thesis's novel approach involved preparing heterogeneous catalysts through pyrolysis and hydrothermal treatment of watermelon rind to create watermelon rind biochar (WB). Subsequently, WB underwent functionalization using HCl, H<sub>2</sub>SO<sub>4</sub>, and H<sub>3</sub>PO<sub>4</sub> at concentrations of 1.6, 3.2, and 4.8N, respectively, at temperatures of 150 °C. These treated WB samples, identified as xWB<sub>y</sub> (where x denoted acid used and y indicated concentration), served as acidic heterogeneous catalysts. To observe catalytic performance, 0.2 g of biochar catalyst and fructose 40 w/v% were mixed with 30 mL of DI water in autoclave reactor, maintaining temperature of 160 °C for 90 mins. Characterization of pristine and functionalized biochar samples was conducted using Field emission scanning electron microscopic (FESEM), N<sub>2</sub> adsorption/desorption, elemental analysis, Fourier transform infrared spectroscopy (FTIR), and Ammonia-temperature programmed desorption (NH<sub>3</sub> – TPD). Findings revealed that pristine biochar treated with 4.8N sulfuric acid displayed a combination of microstructural and mesoporous properties, possessing specific surface area of 464 m<sup>2</sup>/g and pore volume of 0.33 cm<sup>3</sup>/g. Additionally, successful incorporation of acidic functional groups, particularly sulfonic groups, was observed, enabling them to act as acids and facilitate proton transfer to fructose molecules, producing 5-HMF. Quantity of acidity, confirmed via NH<sub>3</sub>-TPD analysis, measured at 4.31 mmol/g. These catalysts provided fructose conversion of 72.3% along with the highest 5-HMF yield and selectivity of 46% and 63%, respectively. Functionalized biochar showed significant potential in utilizing a cost-effective and efficient catalyst derived from agricultural sources for 5-HMF production.

Field of Study: Chemical Engineering

Student's Signature

Academic Year: 2023

.....  
Advisor's Signature

Year:

.....

## ACKNOWLEDGEMENTS

Firstly, I wish to express my sincere gratitude to my advisor, Prof. Dr. Tawatchai Charinpanitkul, from Department of Chemical Engineering, Chulalongkorn University, for his unwavering support throughout this endeavor. His encouragement and opportunity to work at NANOTEC have been invaluable in my personal and professional development.

I am grateful to Dr. Sanchai Kuboon of National Nanotechnology Center (NANOTEC) for creating supportive and friendly work environment and for guiding me to enhance my confidence.

Special thanks to Asst. Prof. Dr. Charusluk Viphavakit for granting me privilege to work in her laboratory.

I am indebted to Dr. Giang T. T. Le for generously sharing insights and assisting me throughout my work.

My appreciation extends to TRG members, particularly Ritikiat Wandaw, for their collaborative contributions during our group meetings.

I want to thank committee members, Asst. Prof. Dr. Palang Bumroongsakulsawat and Asst. Prof. Dr. Chalida Klaysom, for their invaluable guidance during both proposal examination and the defense thesis examination.

I thank the Ratchadpisek Sompoch Fund for their financial support, as well as Chulalongkorn University, and NANOTEC for providing necessary equipment.

Lastly, I am immensely grateful to my father, mother, and brother for their unwavering support throughout my journey.

Pimlapas Bunwichian

## TABLE OF CONTENTS

	<b>Page</b>
ABSTRACT (THAI) .....	iii
ABSTRACT (ENGLISH).....	iv
ACKNOWLEDGEMENTS .....	v
TABLE OF CONTENTS .....	vi
CHAPTER1 .....	1
1.1 Motivation.....	1
1.2 Objective.....	2
1.3 Scope.....	2
1.3.1 Synthesis of xWBy .....	2
1.3.2 Characterization of xWBy.....	2
1.3.3 Investigation of catalytic performance.....	3
1.4 Implementation plans.....	3
1.5 Expectation benefits.....	4
CHAPTER2 .....	5
2.1 5-Hydroxymethylfurfural (5-HMF).....	5
2.2 Reaction pathway of 5-HMF formation from fructose .....	5
2.3 Type of acidic catalyst.....	8
2.3.1 Lewis acid .....	8
2.3.2 Brønsted acid .....	8
2.4 Acidic heterogeneous catalyst .....	9
2.5 Chemical modification of biochar .....	10
2.5.1 Hydrochloric acid (HCl) .....	10
2.5.2 Sulfuric acid (H <sub>2</sub> SO <sub>4</sub> ).....	11
2.5.3 Phosphoric acid (H <sub>3</sub> PO <sub>4</sub> ).....	12
2.6 Literature review.....	12



2.6.1 Preparation of biochar.....	13
2.6.2 Synthesis of functionalized biochar.....	13
2.6.3 Reaction condition.....	16
CHAPTER3 .....	18
3.1. Material and chemicals .....	18
3.2 Preparation of watermelon rind biochar.....	18
3.3 Preparation of functionalized biochar.....	18
3.4 Catalytic characterization.....	18
3.5 Catalytic performance test.....	21
CHAPTER4 .....	23
4.1 Preparation of pristine biochar (WB) from dried watermelon rind by pyrolysis .....	23
4.2 Effect of acid treatment on characteristics of treated biochar .....	28
4.2.1 Chemical compositions, Yields, and Ash.....	28
4.2.2 Surface morphology.....	29
4.2.3 Specific surface area, pore volume, and pore width.....	30
4.2.4 Surface functional groups .....	32
4.2.5 Total acidity.....	35
4.3 Catalytic performance of each acid-treated biochar .....	37
4.4 Effect of sulfuric acid concentration on characteristics of sulfonated biochar .	40
4.4.1 Chemical compositions, Yields, and Ash.....	40
4.4.2 Morphology.....	41
4.4.3 Porous properties .....	42
4.4.4 Surface functional groups .....	43
4.4.5 Total acidity strength.....	44
4.5 Catalytic performance of sulfonated biochar .....	46
CHAPTER5 .....	51
5.1 Preparation of pristine biochar from dried watermelon rind.....	51
5.2 Effect of acid treatment on characteristics of acid-treated biochar .....	51

5.3 Effect of sulfuric concentration on characteristics of sulfonated biochar.....	52
5.4 Remaining issues and Recommendations .....	52
REFERENCES.....	53
VITA.....	63



## LIST OF TABLES

Table 1-1 Implementation plan in this research .....	3
Table 2-1 Catalytic performance with different catalyst.....	8
Table 2-2 $S_{BET}$ , $V_p$ , and $D_{avg}$ of pristine biochar and acid treated biochar .....	16
Table 4-1 Product yields, elemental composition, and ash of samples before and after pyrolysis.....	23
Table 4-2 Quantities of specific surface area, pore volume, and pore width of DRW and WB. ....	26
Table 4-3 Results of yields, chemical elements, and ash on effect of type of acids....	29
Table 4-4 Quantities of specific surface area, pore volume, and pore width of samples .....	32
Table 4-5 Acidity strength of WB and functionalized biochar .....	37
Table 4-7 Performance tests of pristine biochar and pristine biochar .....	40
Table 4-8 Product yields, ash, and chemical contents in sulfonated biochar.....	40
Table 4-9 Physical properties of sulfonated biochar .....	43
Table 4-9 Total acidity strength of sulfonated biochar .....	45
Table 4-10 Catalytic performance of sulfonated biochar.....	46
Table 4-11 Fructose conversion into 5-HMF using various catalyst.....	49

## LIST OF FIGURES

Figure 2-1 Structure of 5-HMF .....	5
Figure 2-2 Schematic of fructose dehydration into 5-HMF.....	6
Figure 2-3 Schematic reaction pathway of conversion fructose into 5-HMF with acid catalyst .....	7
Figure 2-4 Classification of acidity or basicity groups [40] .....	10
Figure 2-5 Reaction pathway of treated biochar with HCl[40].....	11
Figure 2-6 Morphology of pristine WSC and acid treated samples by SEM [51] .....	14
Figure 2-7 FTIR spectra of untreated and treated with acid of watermelon rind[52] .	15
Figure 3-1 Field Emission Scanning Electron Microscope model Quanta FEG 250..	19
Figure 3-2 Micromeritics 3Flex Adsorption analyzer model ASAP2460 .....	20
Figure 3-3 Elemental analyzer model LECO628 series .....	20
Figure 3-4 Fourier transform infrared spectrometer model PERKIN ELMER Spectrum three.....	21
Figure 3-5 MicroActive for AutoChem II 2920 version 6.1 .....	21
Figure 4-1 Surface morphologies of (a, b) DRW, and (c, d) WB.....	24
Figure 4-2 Nitrogen adsorption/desorption isotherm of DWR .....	25
Figure 4-3 Nitrogen adsorption/desorption isotherm of WB .....	26
Figure 4-4 FESEM of functionalized biochar labeled as (a, b) 3.2WBC, (c, d) 3.2WBS, and (e, f) 3.2WBP.....	30
Figure 4-5 N <sub>2</sub> adsorption/desorption isotherms of functionalized biochar .....	31
Figure 4-6 FTIR spectra of pristine and functionalized biochar .....	34
Figure 4-7 NH <sub>3</sub> -TPD results for pristine biochar and functionalized biochar. ....	35
Figure 4-8 Liquid product from fructose dehydration using absence and presence biochar catalysts (a) fructose, (b) Blank, (C) WB, (d) 3.2WBC, (e) 3.2WBS, and (f) 3.2WBP.....	38
Figure 4-9 FESEM images of sulfonated biochar at magnifications of 1,500x (a, c, e) and 5,000x (b, d, f) .....	41
Figure 4-10 BET isotherms of sulfonated biochar .....	42
Figure 4-11 FTIR spectra of sulfonated biochar .....	43
Figure 4-12 NH <sub>3</sub> -TPD profile of sulfonated biochar.....	45

## CHAPTER1

### INTRODUCTION

#### 1.1 Motivation

Recently, depletion of fossil fuels has become a severe situation of petroleum and chemical industries. Biorefinery is considered an alternative process for fossil compensation in many countries[1]. Biomass is an abundant and renewable source of cellulosic content (40-60%)[2]. This content of biomass is a promising source of fructose, which can be utilized as feedstock for production of several valuable platform chemicals such as 5-Hydroxymethylfurfural (5-HMF), formic acid (FA), and levulinic acid (LA)[3].

5-HMF is ranked in the top ten beneficial platform chemicals, which can produce various fine chemicals in many industrial fields[4]. It can be applied to produce 2,5 dimethylfuran (an intermediate to produce biofuel), formic acid (additive chemical in polyester production), and levulinic acid (a fine chemical in plasticizers, polymers, and pharmaceuticals)[5-7]. The dehydration of fructose is considered a practical reaction pathway to produce 5-HMF with a high yield and mild conditions [8, 9]. This reaction could occur with or without catalyst[6]. However, the presence of acidic catalyst could accelerate dehydration reaction by decreasing activation energy[10, 11]. Hydrochloric acid (HCl), sulfuric acid (H<sub>2</sub>SO<sub>4</sub>), and phosphoric acid (H<sub>3</sub>PO<sub>4</sub>) have been widely used as homogeneous catalysts in sugar dehydration process for a few decades. They can generate higher 5-HMF yields but might cause corrosion and have limitations in catalyst recycling. Heterogeneous catalysts, such as metal oxide[12], polymer[13], zeolite[14], ion-exchange resin[15], and carbonaceous materials[6, 10], have been developed for ease of separation, reusability, and lower corrosion[16]. Among many solid catalysts above, carbonaceous materials are promising due to their recycling, and effectiveness for 5-HMF formation[17].

Biochar is a carbonaceous and porous material synthesized via pyrolysis, which is a thermal decomposition process in the absence of oxygen at high temperatures [18, 19]. However, this biochar has low tendency in catalytic application due to its limited number of active sites[17]. Many researchers have investigated functionalizing biochar by acid modification to improve their reactive sites[17, 20]. The reactive sites of biochar with acidic functional groups such as carboxylic, hydroxyl, or sulfonic groups accelerated dehydration reaction in 5-HMF production[16].

A lot of biomass waste from agriculture and food industries has been continually generated annually. Watermelon rind is among biomass waste that has been generated tremendously recently. The production of watermelon is 100 million tons per year in worldwide. 30 % of watermelon production generated watermelon rind which could be reused as a sustainable source for biochar and biochemical production[21]. Watermelon rind biochar has a high specific area and porosity which can be used as an effective

catalyst after chemical modification[22]. Limited research studies have demonstrated modified biochar as catalyst for 5-HMF production. The acid treatment of biochar from watermelon rind could form more acidic active sites which is beneficial for 5-HMF production from fructose.

Therefore, this work aims to study different types and concentrations of acid to functionalize watermelon rind biochar as acidic heterogeneous catalysts for converting fructose into 5-HMF. These catalysts can be synthesized by pyrolysis of watermelon rind biochar and functionalization with acid. All catalysts are characterized using different physicochemical methods and tested for catalytic performance in 5-HMF production under designed experimental conditions.

## 1.2 Objective

Objective of thesis aims to synthesize functionalized biochar as an acidic heterogeneous catalyst for utilization in catalytic conversion of fructose to 5-HMF. Effect of three designated acid solutions (HCl, H<sub>2</sub>SO<sub>4</sub>, and H<sub>3</sub>PO<sub>4</sub>) with specified concentrations (1.6, 3.2, and 4.8 N) on conversion of fructose and production yield of 5-HMF has been investigated.

## 1.3 Scope

Scope of this thesis will cover transformation of watermelon rind to functionalize biochar as an acidic heterogeneous catalyst for 5-HMF production from fructose. Effect of types and concentrations of acid will be studied. There are 3 parts of this work, which include syntheses of functionalized biochar as acidic heterogeneous catalyst, observation of their characteristics, and investigation of fructose conversion and 5-HMF yield.

### 1.3.1 Synthesis of xWBy

xWBy were acid heterogeneous catalysts synthesized from pyrolysis of watermelon rind at 600 °C. Then, pristine biochar was treated with various types (HCl, H<sub>2</sub>SO<sub>4</sub>, and H<sub>3</sub>PO<sub>4</sub>) with concentration of 3.2N to observe effectiveness of acid on functionalized biochar. Next, one proficient acid was selected to activate biochar with acid concentrations (1.6, 3.2, and 4.8 N). xWBy such as xWBC, xWBS, and xWBP have been determined types of acid including HCl (C), H<sub>2</sub>SO<sub>4</sub> (S), and H<sub>3</sub>PO<sub>4</sub> (P) respectively. Whereas “x” have been indicated concentrations of acid.

### 1.3.2 Characterization of xWBy

Characterization of xWBy will be analyzed by Field emission scanning electron microscope (FESEM), N<sub>2</sub> adsorption/desorption isotherm, Element analyzer, Fourier transform infrared spectroscopy (FTIR), and Temperature programmed ammonia desorption (NH<sub>3</sub> – TPD).



conversion into 5-HMF																			
Prepare proposal examination																			
Analyze the catalyst characteristic and discuss its quality on influence of types and concentrations of acid																			
Investigate the designated reaction condition on efficient catalyst																			
Evaluate the catalyst performance																			
Summarize all experimental and analytical results																			
Prepare drafted thesis and complete defending examination																			

### 1.5 Expectation benefits

1.5.1 A process of synthesis of pristine biochar from watermelon rind and its treatment with different types and concentrations of acid for producing functionalized biochar as acidic heterogeneous catalysts.

1.5.2 Physicochemical properties of synthesized acidic heterogeneous catalyst

1.5.3 5-HMF production from fructose using functionalized biochar as acidic heterogeneous catalysts under designed experimental conditions.



## CHAPTER 2

### FUNDAMENTAL KNOWLEDGE

#### 2.1 5-Hydroxymethylfurfural (5-HMF)

5-HMF ( $C_6H_6O_3$ ) consists of furan ring with carbonyl and alcohol groups, as shown in Figure 2-1. 5-HMF is widespread attention as platform chemical due to its wide application to utilized as platform chemical to produce fine chemical (Levulinic acid) biofuel (2,5 dimethylfuran), or polymer (Formic acid)[23]. However, synthesis of 5-HMF from petroleum industry is limited by depletion of fossil, and many researchers have studied to generate this chemical from biomass.

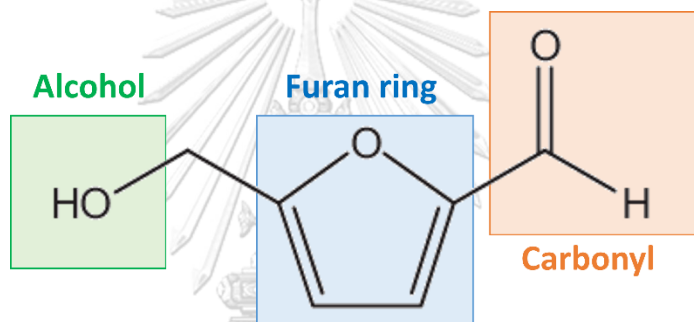


Figure 2-1 Structure of 5-HMF

5-HMF could be synthesized by dehydration of sugar C6 carbon such as sucrose, glucose, and fructose[24], which is obtained from lignocellulosic contents of biomass-derived. In comparison of glucose with fructose, and sucrose as a substrate in the rate of 5-HMF formation, fructose was 31.2 times faster than glucose while sucrose was 18.5 times faster than glucose. Moreover, fructose could inhibit side reactions whereas glucose and sucrose tended to be generated by products such as amino acids[25]. Fructose will be selected as a substrate in this work due to its effective feedstock to produce 5-HMF.

#### 2.2 Reaction pathway of 5-HMF formation from fructose

There are 3 steps of fructose dehydration to form 5-HMF as shown in Figure 2-2. The initiation of dehydration occurs by protonated OH from C2 carbon (1→2→3). The second reaction was followed by removal of OH of C3 carbon (3'→4→5). Finally, third dehydration appeared at C4 carbon, and three water molecules were removed from reaction.

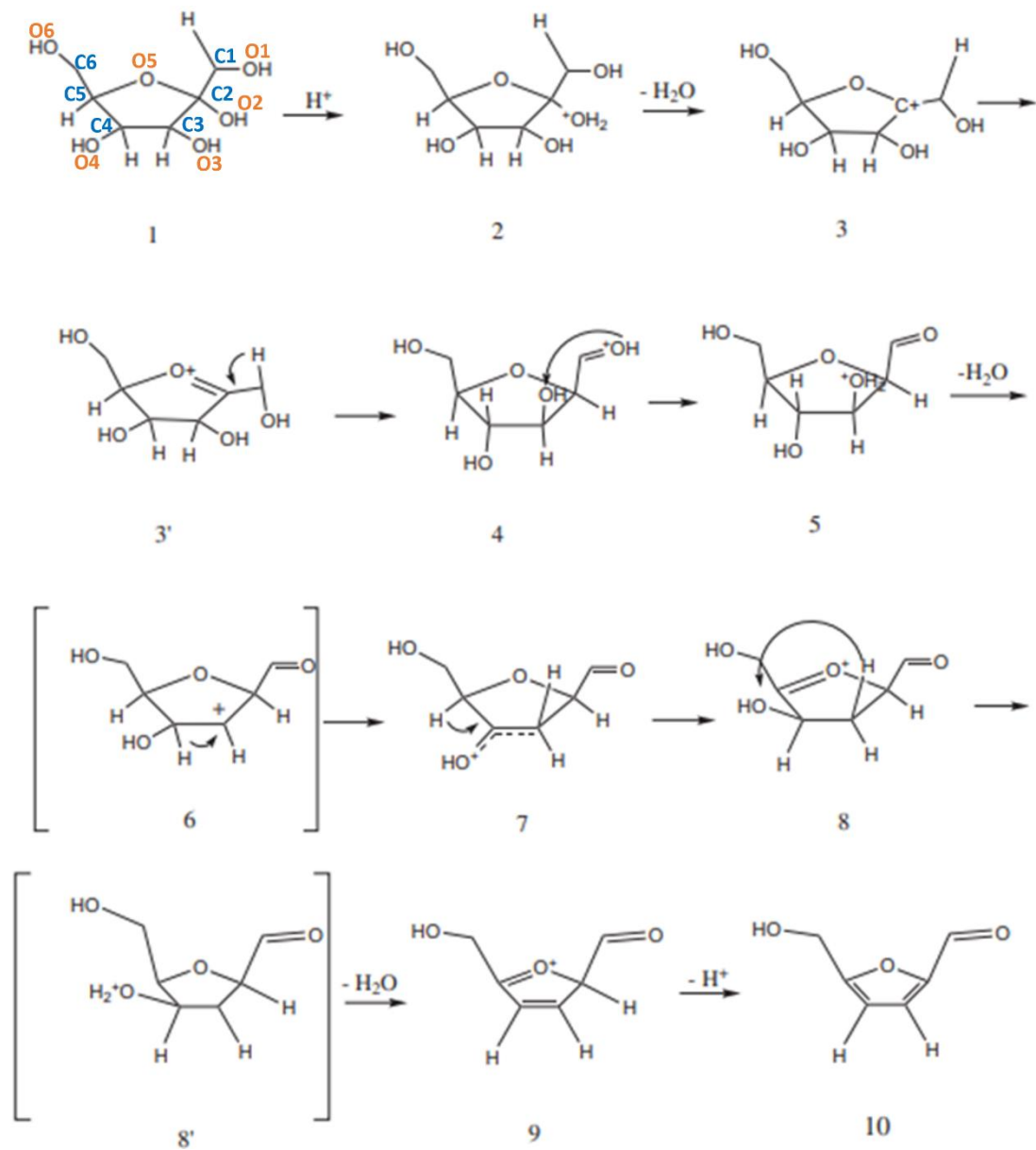


Figure 2-2 Schematic of fructose dehydration into 5-HMF

Meanwhile, many researchers have studied to compare absence with presence of catalysts on 5-HMF formation as follows.

Fructose can be converted to 5-HMF without catalyst called caramelization. The reaction would occur with extreme conditions to enhance production yield. The high temperature of 350 °C, and moderate pressure of 100 MPa obtained the 5-HMF yield of 7.5% reported by Aida et al[26, 27].

In case of presence catalyst shown in Figure 2-3a), the proton ions of catalyst activated on OH- ions of fructose to remove water and generate 5-HMF in mild

conditions[28]. However, catalysts could provide side products including levulinic acid(LA), formic acid (FA), furfural or insoluble humin and soluble polymer as shown in Figure 2-3b)[29].

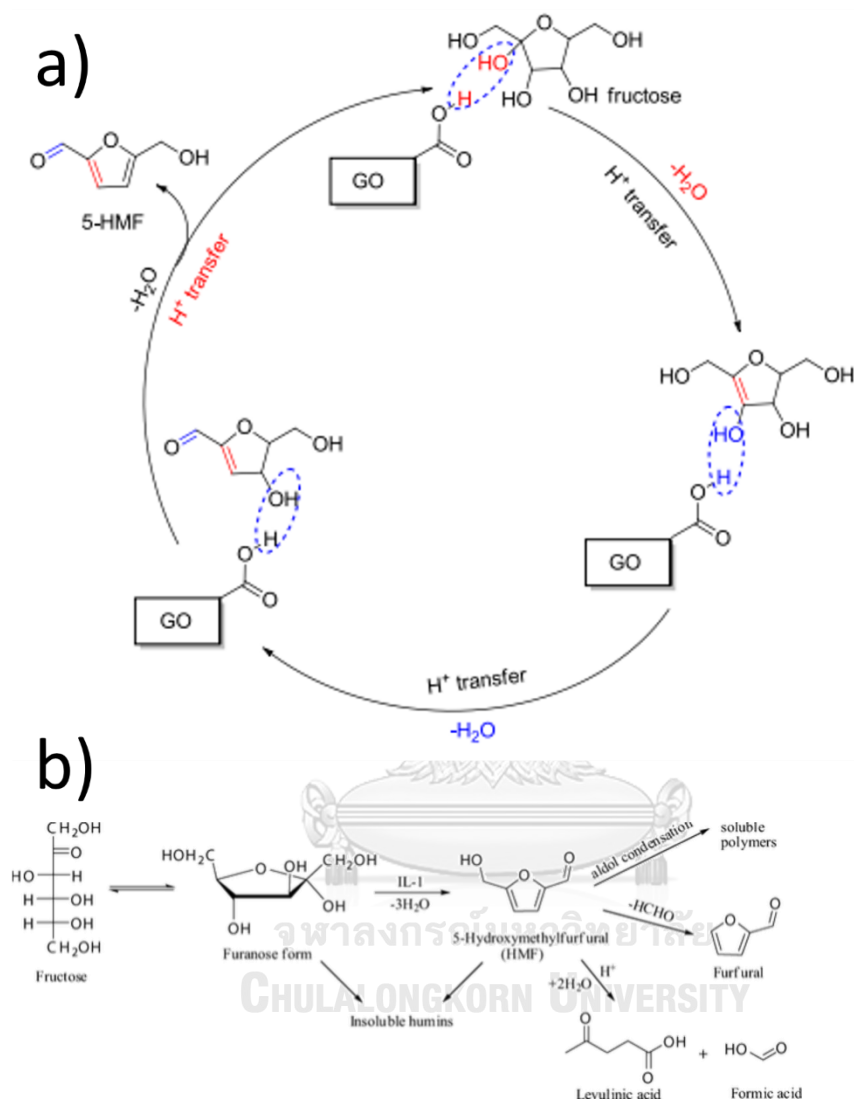


Figure 2-3 Schematic reaction pathway of conversion fructose into 5-HMF with acid catalyst

Compared to the absence or presence of a catalyst, the activation energy ( $E_a$ ) with and without catalysts was 67.5 and 80.1 kJ/mol[11]. These results exposed that catalyst could accelerate dehydration of fructose and increase the formation of 5-HMF. In addition, this work has studied the production of 5-HMF with the presence catalyst, due to its effectiveness, and accessibility of reaction conditions (lower temperature and atmospheric pressure).

## 2.3 Type of acidic catalyst

### 2.3.1 Lewis acid

Lewis acid, called electrophilic, had free space orbital for accepted electron pair. Examples of Lewis catalysts are metal ions such as  $\text{Al}^{3+}$ ,  $\text{Zn}^{2+}$ , or  $\text{Cr}^{2+}$  etc. Catalysts would be used in isomerization reactions for converting glucose into fructose.

### 2.3.2 Brønsted acid

Brønsted acid is a proton donor ( $\text{H}^+$ ) that catalyzes hydrolysis and dehydration of sugars. There are 2 types of Brønsted acid including organic and inorganic acid. Organic acids such as formic acid, acetic acid, lactic acid, oxalic acid, and maleic acid were widely used because of lower poison. These acids can produce 5-HMF yields of 22 to 54 mol% with temperatures of 100 and 150 °C, as discussed in Table 2-1.

Inorganic acid called mineral acid is extensively applied as a catalyst in fructose dehydration due to ease of accessibility, low cost, and strong acid ( $\text{pK}_a \sim -8.0$  to 12.3). According to previous studies, the presence of hydrochloric acid (HCl), sulfuric acid ( $\text{H}_2\text{SO}_4$ ), and phosphoric acid ( $\text{H}_3\text{PO}_4$ ) promoted 5-HMF yields of 53 to 60 %mol as shown in Table 2-1

Table 2-1 Catalytic performance with different catalyst

No.	Catalyst	Reaction condition (solvent, temperature)	5-HMF yield (%mol)	Ref.
1.	Acetic acid	water, 150 °C	44	[30]
2.	Lactic acid	water, 150 °C	50	[30]
3.	Oxalic acid	water, 100 °C	23	[31]
4.	Maleic acid	water, 100 °C	22	[31]

5.	HCl	water, 200 °C	53	[32]
6.	H <sub>2</sub> SO <sub>4</sub>	water, 166 °C	56	[33]
7.	H <sub>3</sub> PO <sub>4</sub>	KBr/MeCN, 160 °C	60	[34]

Although Lewis and Brønsted acid can be used as a catalyst to promote hexose sugars to 5-HMF, Brønsted acid is favored to activate fructose (substrate in this work) dehydration. This work will be studied to use Brønsted acid as a catalyst.

Comparison of organic and inorganic acids with their performance is shown in Table 2-1, This study will use inorganic due to their reactive catalyst and different characteristics (dissociation, chemical elements).

However, Asghari et al. reported that using HCl as homogeneous catalysts (catalyst & substrate: liquid phase) could discover Fe ions in product liquid owing to acid corrosion on equipment[35]. In addition, liquid catalysts could have multiple processes for recycling; heterogeneous catalysts have been proposed to resolve this problem.

#### 2.4 Acidic heterogeneous catalyst

There have been many researches synthesizing acid solid catalysts to enhance the production of 5-HMF by using metal oxide[12], polymer[13], zeolite[14], ion-exchange resin[15], and carbonaceous materials[6, 10]. Among numerous materials, carbonaceous material is promising owing to its renewable source. This material will be studied in this work.

Biochar, prepared from agricultural residue, animal manure, or wood[36], is a carbonaceous material synthesized from thermal decomposition by removing volatile organic compounds under no oxygen at temperatures between 350 to 700°C by pyrolysis[18, 19]. The characteristic of biochar is high specific surface area and porosity due to flexibility of surface improvement. It could be applied as catalyst or absorbent in wastewater.

Nowadays, the watermelon rind production is 30 million tons, generating waste worldwide[21]. Since watermelon rind consists of biopolymers such as pectin, citrulline, cellulose, protein, and carotenoid, which contain acidic functional groups including phenolic [37], hydroxyl (cellulose), and carboxyl (pectin)[38], there would respond to develop for use as acidic catalysts, together with a particular surface area and porous structure of watermelon rind biochar, it will be used as a material in this work [22, 39].

However, the acidic functional groups on watermelon rind biochar were still limited; the enhancement of reactive sites by chemical modification will be studied[17].

## 2.5 Chemical modification of biochar

Presence of oxygen functional groups on biochar surface was considered grafting of acidic or basicity, indicating unique characteristics. Carboxyl, Lactone, Phenol, and Lactol were classified into acidic groups, whereas Chromene, Ketone, and Pyrone were identified as basicity groups [40], illustrated in Figure 2-4. However, original functional biochar groups are restricted, and chemical modifications have been used to improve their properties. Treatments of biochar using HCl, H<sub>2</sub>SO<sub>4</sub>, and H<sub>3</sub>PO<sub>4</sub> were described as follows.

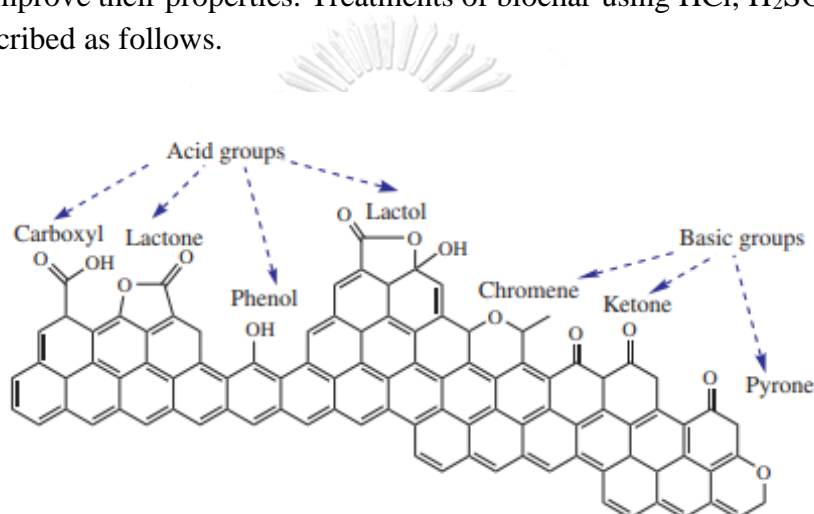


Figure 2-4 Classification of acidity or basicity groups [40]

### 2.5.1 Hydrochloric acid (HCl)

HCl is a strong acid classified as monoprotic, implying it can donate one proton (H<sup>+</sup>) in chemical reaction. Dissociation constant (K<sub>a</sub>) for this reaction is approximately 10<sup>8</sup> (pK<sub>a</sub> = -8)[41]. Dissociation of HCl in water could be represented by Eq. 2-1. H<sup>+</sup> and Cl<sup>-</sup> denoted proton and chloride ion, respectively[42].



As reported by Chen and Wu[43] and depicted in Figure 2-5, the possible mechanism of HCl-treated biochar involved formation of pyrone-type biochar structures. These structures consist of two oxygen atoms with one basic site (ketone). Positioning of oxygens atoms favored for resonance stabilization of positive charge (H<sup>+</sup>). Consequently, when HCl solution, dissociated with higher proton concentration, is applied, it only increases single-bond oxygen functional groups, such as phenol or lactone. It does not generate new functional group. Additionally, acid treatment could remove some small minerals from biochar[40].

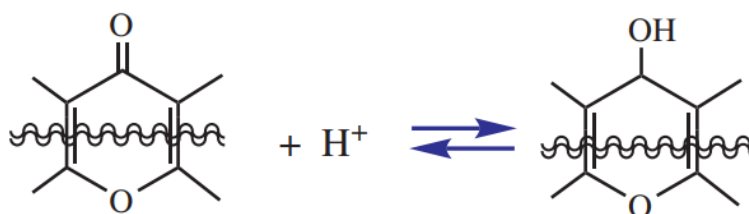
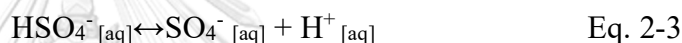
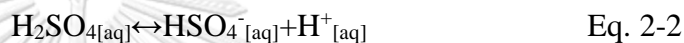


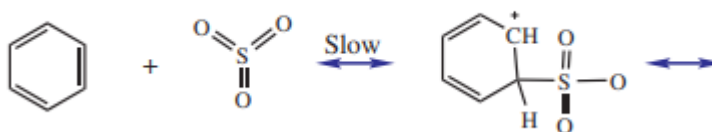
Figure 2-5 Reaction pathway of treated biochar with HCl[40]

2.5.2 Sulfuric acid (H<sub>2</sub>SO<sub>4</sub>)

H<sub>2</sub>SO<sub>4</sub> is a strong diprotic, which dissociated twice, as displayed in Eq. 2-2, 2-3[43]. Values of K<sub>a</sub> for these 2 dissociations are 10<sup>3</sup> and 1.02 x 10<sup>-2</sup> (pK<sub>a</sub> = -3, 1.99)[41], respectively.



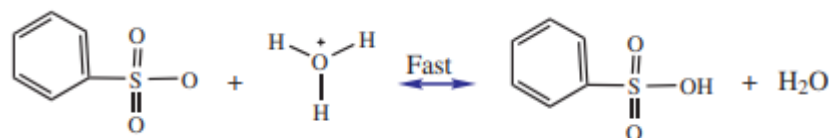
Typically, sulfonation of biochar could be achieved by using fuming sulfuric acid, which produced small molecules of sulfur trioxide (SO<sub>3</sub>). SO<sub>3</sub> is highly reactive electrophile due to presence of electronegative oxygen atoms, allowing it to readily attach to aromatic structure, resulting in sulfonic groups (HSO<sub>3</sub>). Sulfonation process involves several steps. First, SO<sub>3</sub> was generated after heating sulfuric acid (Eq. 2-4). Then, SO<sub>3</sub> sulfonated aromatic compounds to utilize sigma complexes (Eq. 2-5). Protons were removed from the sigma complex to restore aromatic structure (Eq. 2-6). Oxyanions then serve as proton donor (Eq. 2-7)[40].



Eq. 2-5



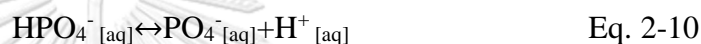
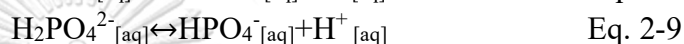
Eq. 2-6



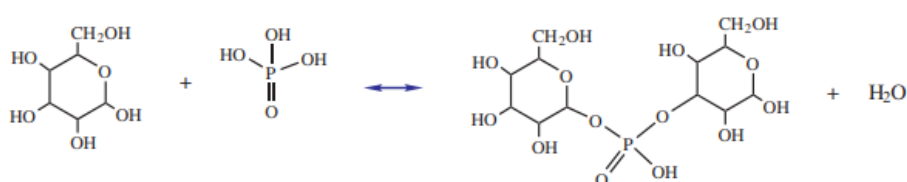
Eq. 2-7

### 2.5.3 Phosphoric acid (H<sub>3</sub>PO<sub>4</sub>)

Compared to HCl and H<sub>2</sub>SO<sub>4</sub>, H<sub>3</sub>PO<sub>4</sub> is the weakest acid, being triprotic and dissociating three times, as displayed in Eq. 2-8, 2-9, and 2-10[44]. Values of K<sub>a</sub> for these three dissociations are 7.59 x 10<sup>-3</sup>, 6.17 x 10<sup>-8</sup>, and 4.79 x 10<sup>-13</sup> (pK<sub>a</sub> = 2.12, 7.21, and 12.32) [41], respectively.



H<sub>3</sub>PO<sub>4</sub> promotes a cleavage of ether groups within lignocellulosic components. This bond cleavage happens concurrently with reactions such as dehydration, degradation, release of CO, CO<sub>2</sub>, and CH<sub>4</sub>, as well as reduction from decomposition of lignin and cellulose, resulting in formation of ketone. The release of CH<sub>4</sub> is attributed to degradation of aliphatic groups and increase in aromaticity Phosphorus compounds link with OH groups on cellulose, crosslinking with polymer chain, with P-containing in center of carbon matrix, as depicted in Eq 2-11[40]. Additionally, carbon from cellulose could be oxidized by acid solution, resulting in creation of new functional groups such as P-O-P and P=O.



Eq. 2-11

Because each acid has unique properties that influence biochar characteristics, the chemical modification on watermelon rind biochar surface with each acid was investigated.

## 2.6 Literature review

In recent years, there has been significant research on preparing biochar as a catalyst to enhance production of 5-HMF from fructose. Researcher has evaluated various parameters for an effective catalyst and studied their impact on 5-HMF yield. Among these parameters, alternative solutions for synthesizing catalysts and optimal



conditions for achieving a higher 5-HMF yield have been explored in many studies, as detailed below.

### 2.6.1 Preparation of biochar

Hao et al. (2022) synthesized sulfonated carbon from discarded masks with 30%  $\text{H}_2\text{O}_2$  at pyrolysis temperature of 400 or 600°C. Results showed that an increase in pyrolysis temperature led to grafting oxygen functional groups (-COOH and -OH) on catalyst surface, promoting higher 5-HMF yield[45].

Leichang et al. (2018) investigated effects of pyrolysis temperature (400-600 °C) and concentrations of acid (0.5, 1, and 2 M) on development of surface area and acidity in pine wood biochar using  $\text{H}_3\text{PO}_4$ . The results reported that temperature of 600 °C and concentration of 2 M yielded the highest specific area and acidity, leading to the highest 5-HMF yield[46].

Wang et al. (2014) conducted a study to prepare solid catalyst from phosphorylated ordered mesoporous carbon by activating it with  $\text{H}_3\text{PO}_4$  at temperatures of 400, 600, and 800 °C. It discovered that carbonization temperature influenced grafting of P-containing compounds onto surface. Temperature of 600 °C remarkably enhanced acidity to 1.12 mmol/g[47].

Krishnan et al. (2023) studied carbonization temperature of dried watermelon rind in range of 500°C to 900°C. It found that temperature of 600°C provided the highest specific surface area of 1216 m<sup>2</sup>/g.

The increase in pyrolysis temperature contributed to enhancement of the specific surface area and presence of acidic functional group on catalyst surface. Pyrolysis temperature of 600 °C will be employed to synthesize watermelon rind biochar in this study.

### 2.6.2 Synthesis of functionalized biochar

Peiris et al. (2019) modified tea-waste biochar using different pyrolysis temperatures (300, 500, and 700 °C) and various types of acids ( $\text{HCl}$ ,  $\text{H}_2\text{SO}_4$ , and  $\text{HNO}_3$ ) to investigate their effects on biochar properties. The results showed that as pyrolysis temperature increased, the amount of acid functional group on biochar surface decreased. Conversely, after treating samples with acid, there was an increase in grafting of acidic functional group on biochar surface[48].

Xiong et al. (2018) reported that wood-wasted-derived had negligible surface acidity. After acid treatment with  $\text{H}_2\text{SO}_4$ , sulfonated wood waste biochar exhibited an increase in total acidity to 0.658 mmol/g and in sulfonic groups to 0.196 mmol/g.

However, specific surfaces decreased due to collapse of mesopores, resulting in formation of micropores[10].

Mengsite et al. (2020) synthesized sulfonated carbon catalysts from corncob using sulfuric acid with varying concentrations of 98, 96, and 94%. This solid catalyst was employed for 5-HMF formation. These results revealed that sample provided maximum total acidity of 3.5 mmol/g, sulfonic group of 0.61 mmol/g, and sulfur content of 1.87%. The authors reported that presence of sulfonic groups, as well as carboxylic and hydroxyl groups, could potentially be used for 5-HMF production[49].

Tomer et al. (2020) studied the effect of concentration of  $\text{H}_2\text{SO}_4$  (0 – 1 M) on  $\text{TiO}_2$  powder for dehydration of fructose to 5-HMF. The results reported that the difference in acid concentration affected acidic strength. The amount of acidity on the surface of catalyst influenced the 5-HMF yield[50].

Liu et al. (2020) studied to modify walnut shell biochar (WSC) and wood powder biochar (WPC) with 30% acid and alkali. The morphology results of WSC treated with  $\text{H}_2\text{SO}_4$  and  $\text{H}_3\text{PO}_4$  showed in Figure 2-6. After being treated with acid, the porosity of biochar was rarely observed because of acidic corrosion[51].

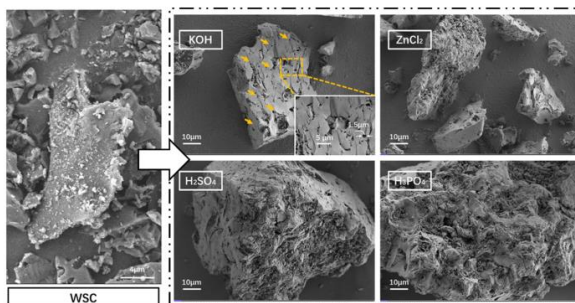


Figure 2-6 Morphology of pristine WSC and acid treated samples by SEM [51]

Kiew et al. (2018) reported that FTIR spectra of untreated and treated  $\text{H}_2\text{SO}_4$  of watermelon rind biochar are shown in Figure2-7. The wavenumber of treated samples around 1419 and 1247  $\text{cm}^{-1}$  assigned the phenolic and carboxylic acid[52].

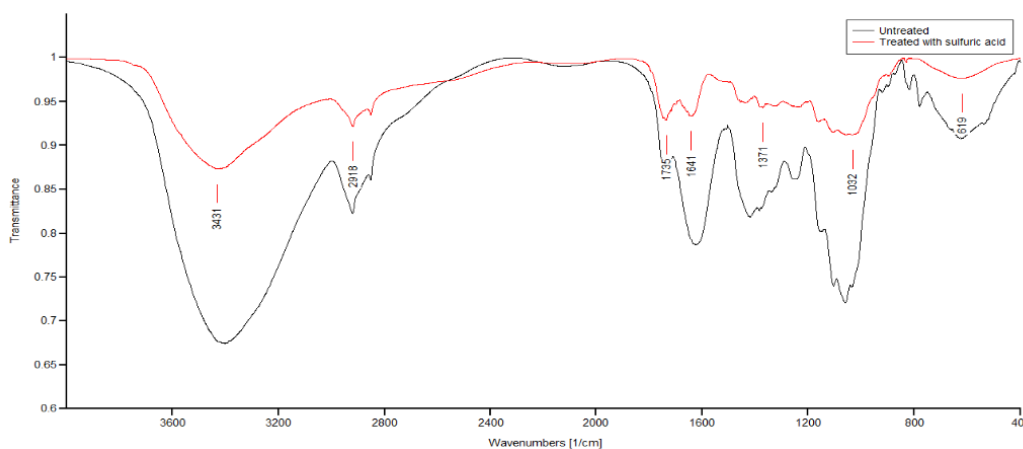


Figure 2-7 FTIR spectra of untreated and treated with acid of watermelon rind[52]

Pande et al. (2018) studied modification of H-USY zeolite by treating it with  $\text{H}_2\text{SO}_4$  and  $\text{H}_3\text{PO}_4$  (10-30 wt%) for 5-HMF formation. Different types of acid and concentrations of acid to catalyst treatment displayed the individual total acidity of catalyst. The results showed that H-USY zeolite modified with 10 wt%  $\text{H}_3\text{PO}_4$  (3.21 N) promoted the most effective catalyst for forming 5-HMF[53].

Leichang et al. (2018) investigated synthesis of biochar from pine wood using  $\text{H}_3\text{PO}_4$  activation at various concentrations (1.5, 3, and 6 N). They observed that samples treated with 6 N had the highest specific surface area of  $1547 \text{ m}^2/\text{g}$ . Moreover, they noted presence of acidic functional groups, including carboxylic, carbonyl, hydroxyl, and oxidized phosphorus groups, which were confirmed by FTIR results. Quantity of acidity was measured at  $3.6 \text{ mmol/g}$ [46].

Peng et al. (2017) studied involving pyrolysis of biochar at  $650^\circ\text{C}$ , followed by activation of biochar using  $\text{H}_3\text{PO}_4$ . In comparison with pristine biochar, treated biochar generated an enhancement in acidic functional groups, including carboxylic and hydroxyl groups, as well as specific surface areas, which increased from  $408$  to  $900 \text{ m}^2/\text{g}$ [54].

Almeida et al. (2017) investigated influence of  $\text{H}_3\text{PO}_4$  treatment on guava seed biochar. They found that morphologies of treated samples remained unchanged. However, they observed the presence of acidic groups, such as hydroxyl groups, and emergence of new functional groups, such as P-N[55].

Lima et al. (2021) reported that the suitability of acidic site and porosity on catalyst surface affected 5-HMF yield and fructose conversion. The optimum specific surface area and acidity are  $100 \text{ m}^2/\text{g}$  and  $0.2$  to  $0.3 \text{ mmol/g}$ , respectively[56].

The acidity of catalyst was main factor that affected the dehydration of fructose to 5-HMF. The various types and concentrations of acid could contribute to grafting of oxygen functional groups on active sites of catalyst surface. However, the effects of different types and concentrations of acid on functionalized biochar and their consequent influence on 5-HMF formation are still limited.

The effect of various types of acid treatment on biochar to specific surface area was reported by Chang et al. [57], Zeng et al. [58], and Kim et al. [59], as shown in Table 2-2. Biochar treated with acid employed the higher specific area than the pristine biochar.

### 2.6.3 Reaction condition

Sonsiam et al. (2019) reported that the increase in reaction temperature and reaction time displayed key factors of 5-HMF yields and fructose conversion. The highest 5-HMF yield was obtained at 120°C for 30 mins[60].

Xiong et al. (2018) studied that wood waste-derived sulfonated with 30 w/v% H<sub>2</sub>SO<sub>4</sub> could employ acid catalyst for production of 5-HMF from fructose in water. The results showed that the temperature in range of 160-180 ° obtained the maximum 5-HMF yield of 42.3%. The increasing temperature could accelerate the dehydration reaction and affect the product yield[10].

Giang et al. (2021) studied to synthesis of magnetic carbon nanoparticles from eucalyptus oil and functionalized them with sulfuric acid in water solvent. The reaction condition was investigated by varying reaction time, temperature, and mass ratio (catalyst: fructose). The result showed that the highest 5-HMF yield (51%) occurred at temperature of 180°C, mass ratio of 0.167, and reaction time of 30 mins[16].

Table 2-2  $S_{BET}$ ,  $V_p$ , and  $D_{avg}$  of pristine biochar and acid treated biochar

Sample	Type of feedstock	Pyrolyzed temperature (°C)	Type of acid	$S_{BET}$ (m <sup>2</sup> /g)	$V_p$ (cm <sup>3</sup> /g)	$D_{avg}$ (nm)	Ref.
550H	Peanut shell	550	-	245.57	0.03	3.14	[57]
HC			1M of HCl	271.90	0.08	2.31	

EC	Eucalyptus twig and leave	500	-	253.35	1.27	21.75	[58]
AC			4.5M of H <sub>2</sub> SO <sub>4</sub>	1265.56	1.31	3.91	
BPB	Banana peel	600	-	11.32	0.027	-	[59]
PBPB			2.3 M of H <sub>3</sub> PO <sub>4</sub>	27.41	0.032	-	



จุฬาลงกรณ์มหาวิทยาลัย  
CHULALONGKORN UNIVERSITY

## CHAPTER 3

### METHODOLOGY

#### 3.1. Material and chemicals

Watermelon rind was selected as a raw biomass and collected from Ratchathewi market in Bangkok, Thailand. Hydrochloric acid (37%, HCl, QRëC), Sulfuric acid (98%, H<sub>2</sub>SO<sub>4</sub>, QRëC), and Phosphoric acid (85%, H<sub>3</sub>PO<sub>4</sub>, QRëC) were used to modify biochar samples. D(-)-Fructose (C<sub>6</sub>H<sub>12</sub>O<sub>6</sub>, KEMAUS) was used as a substrate for 5-HMF production.

#### 3.2 Preparation of watermelon rind biochar

Watermelon rind was cut, washed with deionized water (DI) twice, and then dried in an oven at 100 °C for 72 h to remove water. Dried watermelon rind (DRW) was subsequently ground and sieved to size of less than 300 µm. Watermelon rind powder was pyrolyzed at 600 °C for 2 h in absence of oxygen using quartz-tube furnace. This reaction was maintained in at constant flow rate of N<sub>2</sub> (50 mL/min) and constant heating rate (5°C/min). After cooling down, pristine watermelon rind biochar (WB) was obtained.

#### 3.3 Preparation of functionalized biochar

1 g of WB underwent acid treatment using 20 mL of acid solutions (HCl, H<sub>2</sub>SO<sub>4</sub>, and H<sub>3</sub>PO<sub>4</sub>) with concentrations of 1.6, 3.2, and 4.8 N in Teflon-line container. Subsequently, dispersed solutions were stirred with sonication for 15 mins. Samples were placed in hydrothermal reactor and heated to 150 °C for 24 h. Afterwards, treated samples were washed with aqueous media to remove excessive acid solutions until pH reached neutrality and were dried in an oven overnight. Functionalized samples of xWBy served as acidic heterogeneous catalysts. Letter “y” were representing types of acids used, which include C (HCl), S (H<sub>2</sub>SO<sub>4</sub>), and P (H<sub>3</sub>PO<sub>4</sub>), respectively. “y” denoted concentrations of acid, such as 1.6, 3.2, and 4.8.

#### 3.4 Catalytic characterization

Surface morphologies of xWBy

Surface morphologies of xWBy were visualized by Field Emission Scanning Electron Microscope (FESEM, Quanta FEG 250, The Netherlands) at magnifications of 1,500x and 5,000x, as shown in Figure 3-1.



*Figure 3-1* Field Emission Scanning Electron Microscope model Quanta FEG 250

Specific surface area, pore volume, and pore width of xWBy

Specific surface area, pore volume, and pore size of xWBy were determined by Nitrogen adsorption/desorption isotherms (ASAP2460, Micromeritics, Thailand), as illustrated in Figure 3-2. Prior to isotherm analysis, all samples were purged with nitrogen gas at 150 °C for 14 h to remove any moisture or contaminants. N<sub>2</sub> adsorption/desorption isotherms were determined at -196°C. Specific surface area was calculated by Brunauer, Emmett, and Teller equation, established relationship between quantity adsorbed (cm<sup>3</sup>/g STP) and relative pressure (p/p<sup>o</sup>). Pore volume and pore width were gained by BJH desorption method.



*Figure 3-2* Micromeritics 3Flex Adsorption analyzer model ASAP2460

Chemical compositions of xWBy

Elemental compositions (C, H, N, and S) of xWBy were measured using Elemental analyzer (628 series, LECO 628, USA), as shown in Figure 3-3. Percentage of O content was calculated by difference.



*Figure 3-3* Elemental analyzer model LECO628 series

Surface functional groups of xWBy

Surface functional groups of xWBy were identified by Fourier transform infrared spectrometer with UATR (FTIR Spectrum three, PERKIN ELMER, America) shown in Figure 3-4. Machine was performed within a wavelength of 600 to 4,000  $\text{cm}^{-1}$ .





*Figure 3-4* Fourier transform infrared spectrometer model PERKIN ELMER  
Spectrum three

Acidity strength of xWBy

Ammonia temperature programmed desorption (NH<sub>3</sub>TPD) was used to measure total acidity. In this work, 0.03 g of samples were preheated to 200°C for 180 mins and then cooled down to 40°C. All samples were saturated with NH<sub>3</sub>/He at 40°C for 60 mins. After saturation, ammonia was desorbed in a flow of He for 60 mins and waited until baseline was stable. Subsequently, absorbed samples were heated from 40°C to 800°C. Amount of ammonia effluent was detected using MicroActive for AutoChem II 2920 version 6.1 shown in Figure 3-5.



*Figure 3-5* MicroActive for AutoChem II 2920 version 6.1

Amount of ash

Amount of ash can be analyzed using standard test method ASTM D3174. To perform this analysis, 0.05 g of sample was heated up from room temperature to 750°C for 2 h. Percentage of ash in analyzed sample was calculated using following equation, where A, B, and C represented weight of ceramic boat and ash residue (g), weight of empty ceramic boat (g), and weight of analysis sample (g)

$$\text{Percentage of ash (\%)} = [(A-B)/C] \times 100 \quad \text{Eq. 3-1}$$

### 3.5 Catalytic performance test

Experiments were conducted following methodology described by Giang et al. (2021)[16], with some adaptations, displayed in APPENDIX C. Initially, 0.2 g of

sample was mixed with 4 w/v% solution of fructose in 30 mL of DI water within Teflon-lined hydrothermal reactor. Reactor was maintained at constant temperature of 160°C for 90 mins with stirring rate of 200 rpm, controlled by temperature controller. Subsequently, reactor was cooled down with ice to stop dehydration reaction. Liquid products, obtained from experiment, were collected using syringe filter (13 mm, 0.2 µm, Whatman). After filtering, composition of liquid products was analyzed using high-performance liquid chromatography (HPLC) equipped with Aminex sugar column (HPX-87H sugar 300 × 7.8 mm, Bio-Rad, Hercules, CA). Sugar and liquid products were detected using RI detector (RID-10A), and UV-VIS detector (SPD-20AV). Mobile phase, consisting of 5mM sulfuric acid, was used with flowrate 0.6 mL/min at 45 °C for 70 mins. Fructose conversion and product yield were calculated using following equations.  $F_i$ , and  $F_f$  determined concentration of fructose before and after dehydration reaction.

$$\text{Fructose conversion (mol\%)} = \frac{F_i - F_f}{F_i} \times 100\% \quad \text{Eq. 3-2}$$

$$\text{Product yield (mol \%)} = \frac{\text{mol of produced product}}{F_i} \times 100\% \quad \text{Eq. 3-3}$$

## CHAPTER 4

### RESULTS AND DISCUSSIONS

#### 4.1 Preparation of pristine biochar (WB) from dried watermelon rind by pyrolysis

Generally, dried watermelon rind is natural biomass, which contains basic contents of carbon, hydrogen, nitrogen, oxygen, and other trace components. Pyrolysis was employed for preparing pristine biochar samples through the removal of undesirable contents except carbon. In this work, pyrolysis conditions were conducted at 600°C for 2 h, resulting in pristine biochar (WB), which mainly contains carbon with only a few contents of other components. Elemental composition of typical samples before and after pyrolysis were summarized in Table 4-1.

Table 4-1 Product yields, elemental composition, and ash of samples before and after pyrolysis

Samples	Product yield (%)	Ash (%)	Percentage of elements (%)				
			C	H	N	S	O <sup>b</sup>
DWR	-	13.4	36.2	5.2	2.5	0.2	55.9
WB	35.2±2.2 <sup>a</sup>	13.9	52.1	1.2	2.0	0.2	44.5

a: amount of pristine biochar acquired after pyrolysis process at temperature of 600°C.

b: by difference

To observe effect of pyrolysis treatment, characteristics of samples such as chemical elements, yields, and amount of ash were displayed in Table 4-1. Yield of WB was approximately 35.2% after thermal treatment of dried watermelon rind. This yield was a result of evaporation of moisture and light volatile compounds in initial stages (35°C to 100°C) of heating. In subsequent stages, as pyrolysis temperature increased from 100°C to 600°C, it promoted decomposition of hemicellulose (220-315°C), cellulose (315-400°C), and some portions of lignin (160-900°C)[61]. Lignin, which decomposed at high temperatures, was mainly precursor of pyrolytic biochar.

According to thermal treatment, fraction of carbon rose from 36.2% to 52.1%, which was attributed to aromatization and condensation of benzene rings within

lignin[61]. Whereas contents of hydrogen and nitrogen decreased from 5.2% to 1.2% and from 2.5% to 2.0%, respectively. Reduction in hydrogen content could be attributed to removal of H<sub>2</sub>O or hydrocarbons (CH<sub>4</sub>, C<sub>2</sub>H<sub>2</sub>, and C<sub>2</sub>H<sub>4</sub>) during thermal decomposition. Furthermore, degradation of nitrogen could result from disintegration of nitrogen-containing biochar during pyrolysis[62]. Oxygen contents could decrease due to volatilization of polar functional groups, it decreased from 55.9% to 44.5%. Additionally, it observed an increase in ash contents from 13.4% to 13.9%, which loss of impurities during pyrolysis[63]. Presence of ash may involve individual inorganic compounds derived from dried watermelon rind, such as Na<sub>2</sub>O, SiO<sub>2</sub>, P<sub>2</sub>O<sub>5</sub>, SO<sub>3</sub>, MgO, and K<sub>2</sub>O[64].

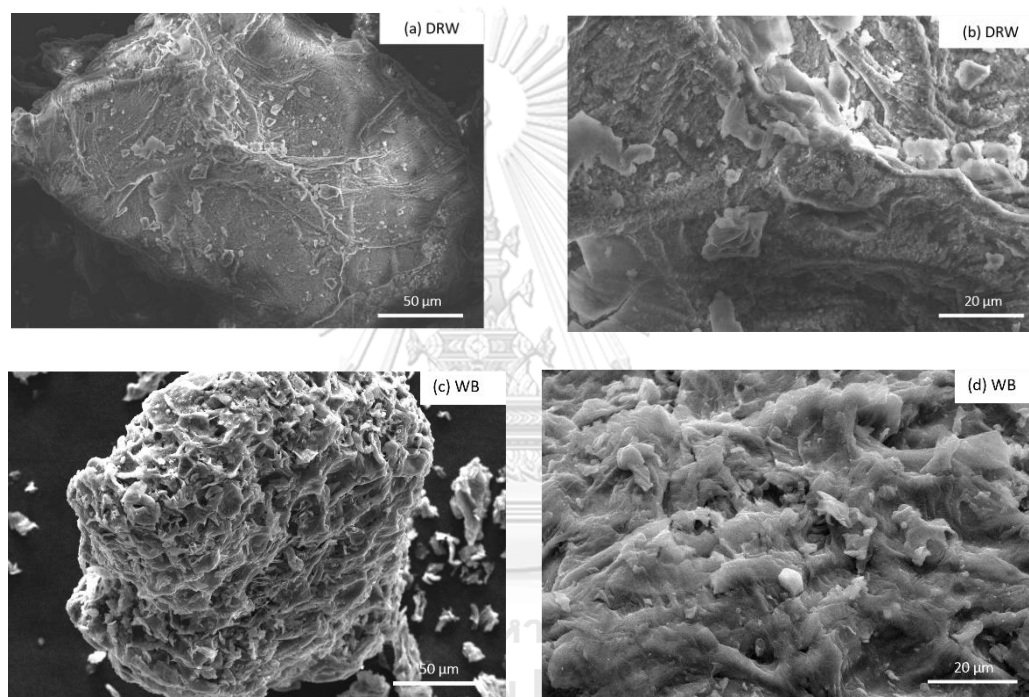


Figure 4-1 Surface morphologies of (a, b) DRW, and (c, d) WB

Surface morphology of DRW and, WB was regarded by FESEM at magnifications of 1,500x, and 5,000x, as shown in Figure 4-1. In Figure 4-1(a, b), DRW observed relatively non-porous structures as reported by Wei et al[65]. According to pyrolysis, WB exhibited a large porous structure, indicating breakdown of lignocellulosic structure, as shown in Figure 4-1(c). To closer inspection in Figure 4-1(d), WB surface was found to be covered with small impurity particles, which were originally compounds of DWR and remained unburned during pyrolysis.

Moreover, generation of porosity after thermal treatment could be confirmed by N<sub>2</sub> adsorption/desorption results as illustrated in Figure 4-2, Figure 4-3, and Table 4-2. BET isotherm, which depicted relationships between quantity adsorbed and relative pressure, was used to explain kind of porosity. BET isotherms of DRW were displayed

in Figure 4-2, isotherm of DRW observed small steep slope near vertical at low relative pressure and then became plateau curve at  $p/p^0$  range of 0.1-0.7, with increase in adsorbed gas as relative pressure increased. This behavior is similar to type II isotherm. It implied that there were non-porous or macroporous structures in DRW[66].

Adsorption curve of WB, shown in Figure 4-3, exhibited continuous increase in quantity of adsorbed gas as relative pressure increased. Desorption curve tended to overlap with adsorption curve. It was demonstrated as a combination of type IV(a) and IV(b) isotherms, implying the entire mesoporous structure.

To confirm presence of porosity,  $S_{BET}$  was calculated using BET method. Pore volume, and pore size were determined using BJH method, which analyzed entire BET isotherm graph, as shown in Table 4-2.

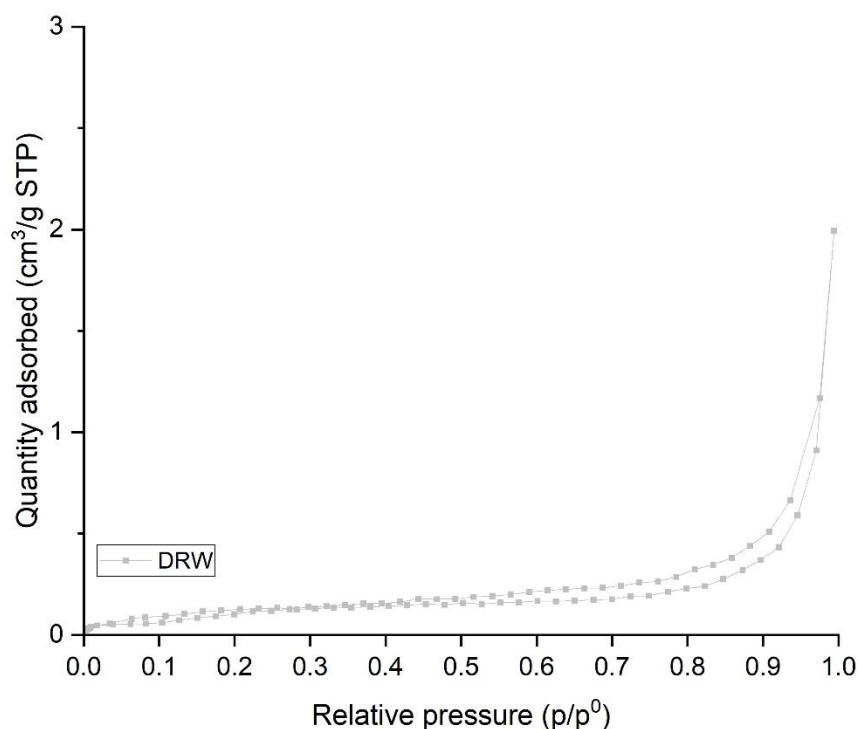


Figure 4-2 Nitrogen adsorption/desorption isotherm of DWR

Quantities of specific surface area ( $S_{BET}$ ), pore volume ( $V_p$ ), and pore width were presented in Table 4-2. Since breakdown of aliphatic bonds and condensation into aromatic linkages during pyrolysis may contribute to increased  $S_{BET}$  and  $V_p$ [63]. The  $S_{BET}$  and  $V_p$  of DWR and WB rose from 0.5 to 394.3  $\text{m}^2/\text{g}$  and from 0.003 to 0.44  $\text{cm}^3/\text{g}$ , respectively. Increase in  $S_{BET}$  and  $V_p$  aligned with previous findings reported by Elnour et al. Their study focused on pyrolysis date palm wasted at 600°C, demonstrating an enhancement in specific surface from 1.0 to 221.2  $\text{m}^2/\text{g}$  and in pore volume from 0.005 to 0.03  $\text{cm}^3/\text{g}$ [67]. During decomposition of biochar, it may lead to formation of small

pores which could be attributed to opening of pores. Additionally, evaporation of light volatile could void a small pore on its surface. As a result, pore size decreased from 25.5 nm to 4.5 nm due to rearrangement of biochar structure.

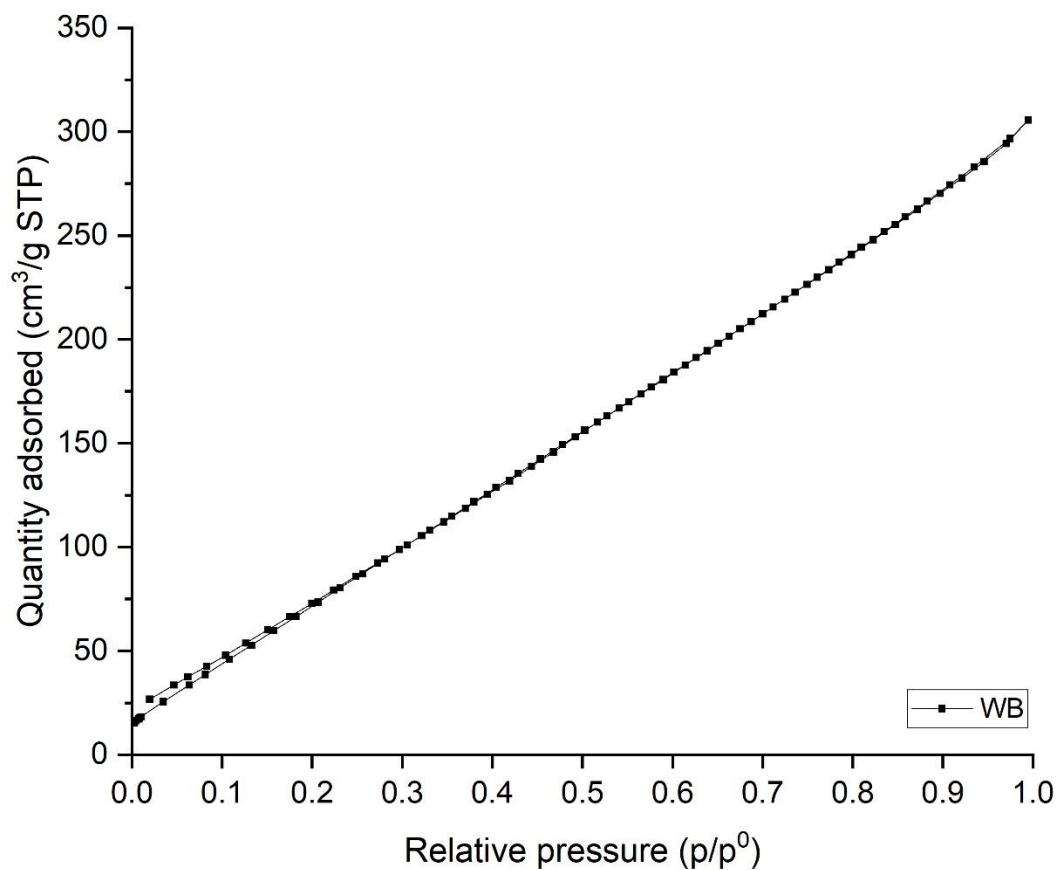


Figure 4-3 Nitrogen adsorption/desorption isotherm of WB

Table 4-2 Quantities of specific surface area, pore volume, and pore width of DRW and WB.

Sample	$S_{BET}$ ( $\text{m}^2/\text{g}$ )	$V_p$ ( $\text{cm}^3/\text{g}$ )	$D_{avg}$ (nm)
DRW	0.5	0.003	25.5
WB	394.3	0.44	4.5

Based on results, it was evident that pyrolysis pretreatment of watermelon rind biochar could affect its chemical elemental composition and improve porosity of biochar surface.



## 4.2 Effect of acid treatment on characteristics of treated biochar

Effect of acid treatment on characteristics of biochar samples treated with 3 different types of acid solutions, HCl, H<sub>2</sub>SO<sub>4</sub>, and H<sub>3</sub>PO<sub>4</sub> with a designated concentration of 3.2 N was experimentally examined. Typical samples of biochar treated with HCl was denoted as 3.2WBC, biochar treated with H<sub>2</sub>SO<sub>4</sub> was 3.2WBS, and biochar with H<sub>3</sub>PO<sub>4</sub> was 3.2WBP. Characteristics of acid-treated biochar, which were chemical compositions, morphology, specific surface area, surface functional groups, and total acidity were discussed in the following sections.

### 4.2.1 Chemical compositions, Yields, and Ash

Natural acid dissociation results in generation of proton ions and anions. Concentration of these ions depends on a linear relationship with acid dissociation constant and concentration of acid used. Both protons and anions could influence biochar properties during acid treatment. Proton ions can corrode biochar surface and remove impurities. On the other hand, anions might introduce new functional groups onto biochar surface. The specific changes in biochar characteristics were discussed as follows.

Generally, pristine biochar may contain by-products, acquired from pyrolysis, including ash, and minerals. Mineral compounds, which are predominantly hydrophilic, and ash could easily dissolve in water[68]. Hence, these compounds could be removed using acid solution, resulting in reduction in mass of functionalized biochar after acid treatment[69]. In comparison types of acids, HCl, being the strongest acid, exhibited a probability to remove impurity contents from biochar, decreasing mass of functionalized biochar to 51.5% after acid treatment. In contrast, H<sub>2</sub>SO<sub>4</sub> and H<sub>3</sub>PO<sub>4</sub> which were weaker acids compared to HCl, left impurity residue, remained at 60.1% and 66.9%, respectively. However, despite ash removal using acid solution, residual ash content was observed after acid treatment of 3.2WBC, 3.2WBS, and 3.2WBP, which were 2.6%, 2.6%, and 4.1%, respectively (Table 4-3).

Elemental compositions of functionalized biochar were illustrated in Table 4-3. When comparing functionalized biochar to untreated WB, percentage of carbon in treated biochar increased from 52.1% to 74.7% due to reduction of impurities[70]. Reduction of oxygen compound could inverse hydrophilic group to weaker polar group during acid treatment[71]. Nitrogen contents showed unnoticed decrease, likely due to acid corrosion on biochar surface. In contrast, hydrogen content tended to increase due to grafting hydrogen bonds on functional groups on biochar. As a result of varying types of acids used, amounts of C, H, N, and O in samples showed insignificant differences. In case of sulfur, it remained unchanged in 3.2WBC and 3.2WBP samples. However, it significantly increased with sulfuric acid treatment (3.2WBS), due to the grafting of



sulfonic groups from sulfuric acid, and the presence of sulfuric group was confirmed through FTIR results.

Acid treatment had an impact on chemical elements of biochar, likely due to corrosive nature of acid and introduction of new chemical groups in some samples. Interestingly, types of acids used for chemical treatment showed insignificant influence on chemical properties of carbon, hydrogen, oxygen, and nitrogen in functionalized biochar.

Table 4-3 Results of yields, chemical elements, and ash on effect of type of acids.

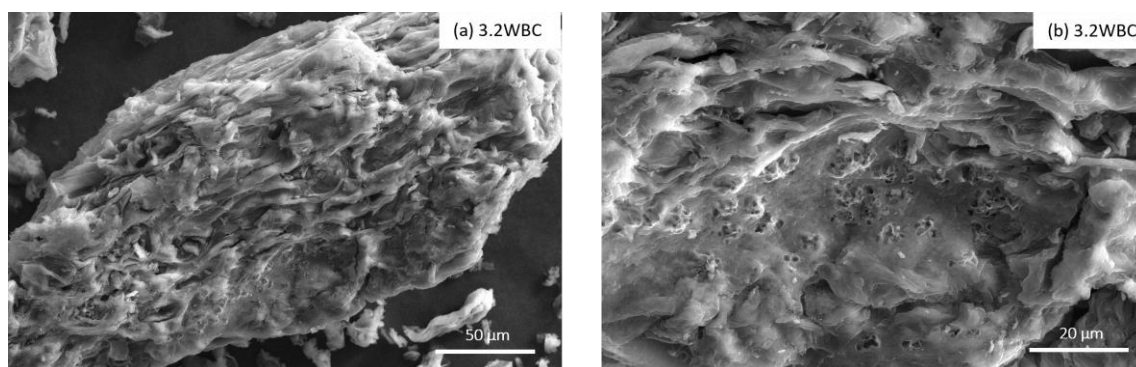
Samples	Product yield <sup>a</sup> (%)	Ash (%)	Percentage of elements (%)				
			C	H	N	S	O <sup>b</sup>
3.2WBC	51.5±1.1 <sup>b</sup>	2.6	74.7	1.9	1.8	0.2	21.4
3.2WBS	60.1±1.8 <sup>b</sup>	2.6	71.8	1.7	1.7	1.9	22.9
3.2WBP	66.9±1.1 <sup>b</sup>	4.1	73.9	1.6	1.5	0.2	22.8

a: amount of activated biochar obtained after chemical modification.

b: by difference

#### 4.2.2 Surface morphology

In Figure 4-4(a, c, e), activated samples (3.2WBC, 3.2WBS, and 3.2WBP) observed a multi-layered pore structure similar to WB. When observed at higher magnification in Figure 4-4(b, d, e), channels became clearly visible due to removal of impurities after acid treatment[51]. Additionally, acid treatment could corrode biochar surface, leading to formation of micropore structures[71].



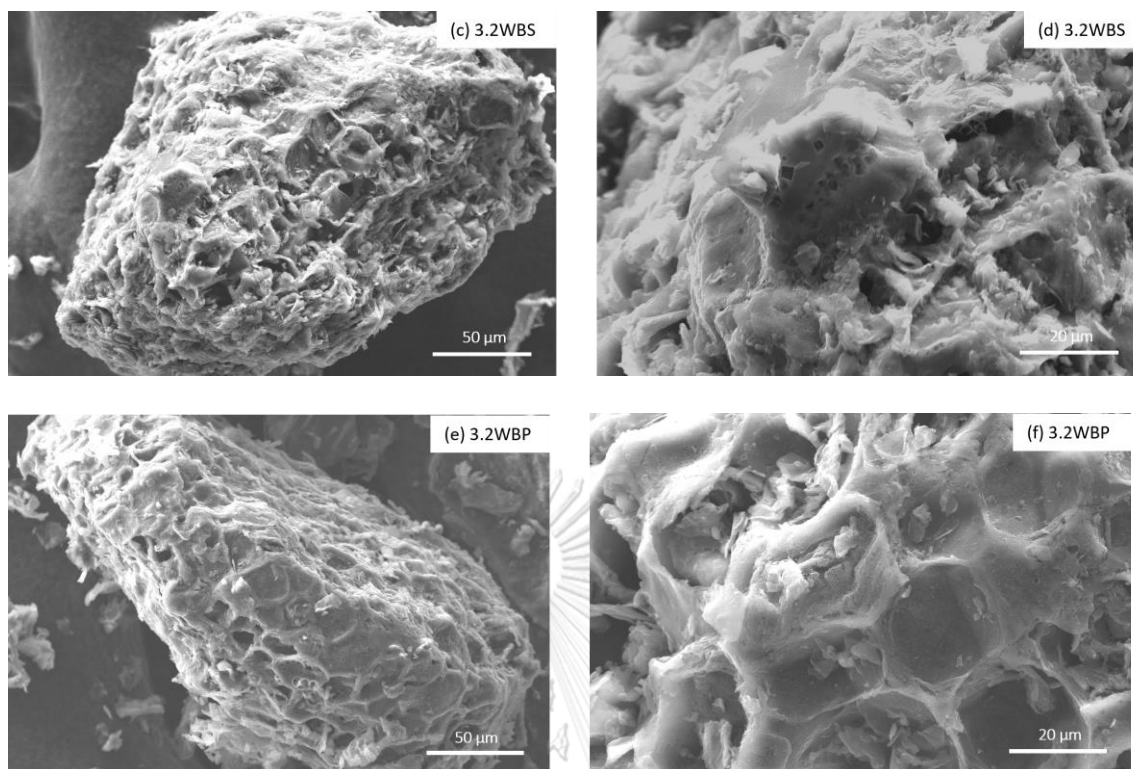


Figure 4-4 FESEM of functionalized biochar labeled as (a, b) 3.2WBC, (c, d) 3.2WBS, and (e, f) 3.2WBP

#### 4.2.3 Specific surface area, pore volume, and pore width

Existence of pore structure, as observed in FESEM images could be confirmed by  $N_2$  adsorption/desorption results, shown in Figure 4-5 and Table 4-4. In Figure 4-5, quantities of adsorption of functionalized biochar were observed to increase rapidly at low relative pressure ( $p/p^0 < 0.003$ ), implying that acid treatment could generate micropore structures[71]. Moreover, hysteresis loop of type IV isotherm, depicted at  $0.4 < p/p^0 < 1$ , implied the presence of mesostructure.

During acid treatment, dissociation of acid likely contributed to removal of impurities that might have been obstructing pore structure. Additionally, acid eroded biochar structure, leading to creation of micropores[57]. Consequently,  $S_{BET}$  of 3.2WBC, 3.2WBS, and 3.2WBP increased to 496.5, 438.7, and 460.2  $m^2/g$ , respectively. This enhancement in specific surface area was confirmed by BET isotherms, indicating that functionalized biochar attained a new microporous structure. Differences in specific surface area among various types of acid treatments were not substantial. When comparing 3.2WBC with other samples, it showed a slightly higher specific surface area due to stronger acidity than HCl. Conversely, while  $H_2SO_4$  and  $H_3PO_4$  exhibited lower acidity than HCl, it resulted in slightly lower specific surface

area.

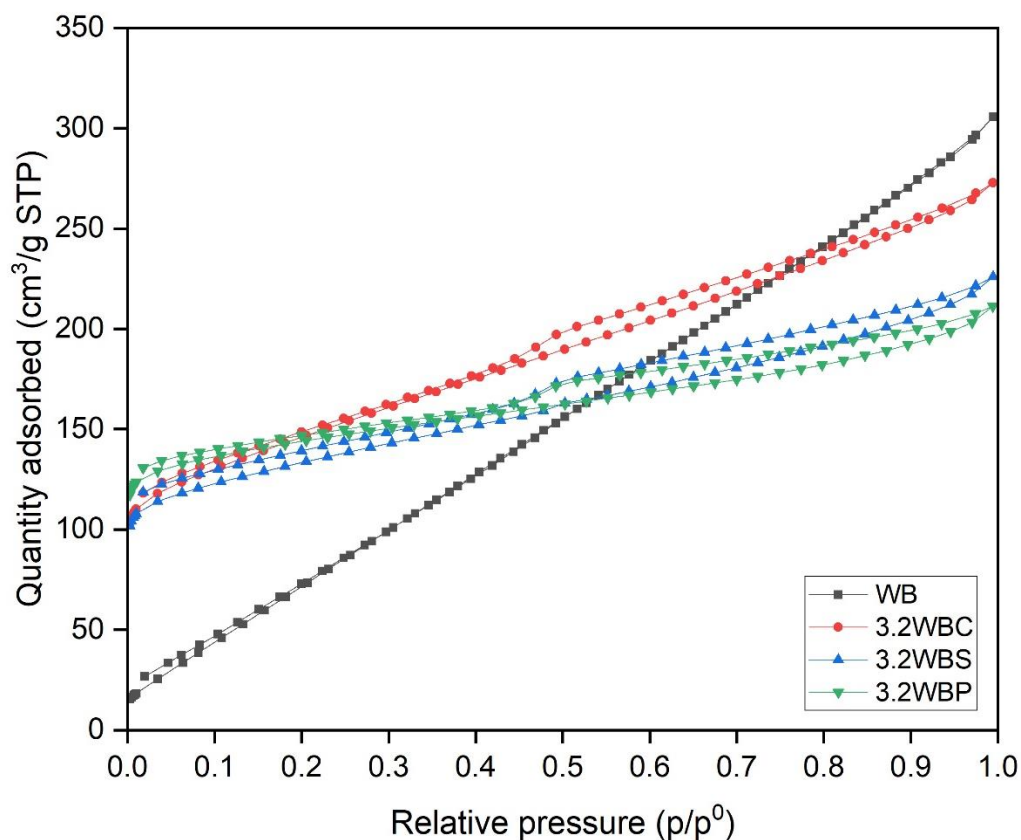


Figure 4-5 N<sub>2</sub> adsorption/desorption isotherms of functionalized biochar

Comparing functionalized biochar with pristine biochar (0.44 cm<sup>3</sup>/g), pore volume of sample treated with HCl was 0.31 cm<sup>3</sup>/g due to generation of micropores. Furthermore, in the 3.2WBS sample, pore volume decreased to 0.21 cm<sup>3</sup>/g due to presence of micropores and potential clogging from sulfate ions. Similarly, pore volume of 3.2WBP sample (0.15 cm<sup>3</sup>/g) showed tendency to decrease due to formation of P-containing compounds, resulting in micropores blockage[55]. Increase in specific surface area and decrease in pore volume aligned with previous work as reported by Zeng et al.[72]. Pore sizes of 3.2WBC, 3.2WBS, and 3.2WBP slightly decreased to 4.2, 4.3, and 4.4 nm, respectively. These values appeared to be close among treated samples.

Table 4-4 Quantities of specific surface area, pore volume, and pore width of samples

Sample	$S_{\text{BET}}$ ( $\text{m}^2/\text{g}$ )	$V_{\text{p}}$ ( $\text{cm}^3/\text{g}$ )	$D_{\text{avg}}$ (nm)
3.2WBC	496.5	0.31	4.2
3.2WBS	438.7	0.21	4.3
3.2WBP	460.2	0.15	4.4

The results indicated that acid modification affected surface and textural properties of biochar. Presence of porosity in functionalized biochar could promote interaction of fructose with acidic sites on catalysts, thereby possibly enhancing 5-HMF production, as reported by Lei chang et al.[46]. When comparing various samples treated with different acids at equivalent concentrations, there was a negligible variation in specific surface area, pore volume, and pore width. However, distinct differences were observed in types of functional groups, as revealed in subsequent analyses.

#### 4.2.4 Surface functional groups

Surface functional groups of samples were determined using FTIR, as illustrated in Figure 4-6. Initially, pristine biochar (WB) contained out-of-plane isolation involving carbon and hydrogen atoms bonding within lignocellulosic contents, observed at  $876 \text{ cm}^{-1}$ [48]. Stretching vibration of aromatic carbon ( $\text{C}=\text{C}$ ) appeared as a peak at  $1615 \text{ cm}^{-1}$ , indicating polymerization of pyrolyzed carbon[73]. Presence of ether in lignin or primary alcohol groups on carbohydrates ( $-\text{CH}_2\text{OH}$ ) was represented by wavelength of  $1019 \text{ cm}^{-1}$ , exclusively observed in WB[74]. Additionally, peak at  $1354 \text{ cm}^{-1}$ , corresponded to in-plane bending of methyl group ( $-\text{CH}_3$ ) vibration bonded in pectin structure[75]. Distinctive peaks at  $1702 \text{ cm}^{-1}$  indicated stretching vibrations of carboxylic or carbonyl ( $\text{C}=\text{O}$ ) groups[76]. Strong signals at  $1235 \text{ cm}^{-1}$  representing stretching bond  $\text{C}-\text{O}$  represented presence of phenol or lactone groups[48]. Pronounced  $-\text{OH}$  stretching was observed at the peak of  $3414 \text{ cm}^{-1}$ , similar to previous work by Li et al. (2019), attributed to exotic oxyacid radical group[75]. Additionally, intensity peak of  $-\text{OH}$  was comparable to previous work reported by Elnour et al.[67].

Compared to original functional groups in WB, FTIR spectra of functionalized biochar exhibited changes in peak intensities and emergence or disappearance of peaks following acid modification. Primary alcohol ( $1019 \text{ cm}^{-1}$ ) and methyl group ( $1354 \text{ cm}^{-1}$ ) vanished in all functionalized samples (3.2WBC, 3.2WBS, and 3.2WBP) due to their affinity for bonding with functional groups, which could dissolve in water.

HCl treatment (3.2WBC) revealed a strong peak of carboxylic or carbonyl groups, as indicated at wavenumber of  $1702\text{ cm}^{-1}$ [77]. This increase in carboxylic content was attributed to generation of chlorine gas from contact of HCl with atmospheric oxygen. Chlorine gas behaves as an oxidizing agent, facilitating oxidation of primary alcohols into carboxylic groups. Furthermore, proton ions could promote disintegration of carbonyl groups, leading to increase in single-bond oxygen functional groups[40], such as lactone or phenol. This showed a broadening of C-O peak in range of  $1084$  to  $1239\text{ cm}^{-1}$ [78, 79]. However, this treatment also retained C=C and C-H peaks due to original biochar structure.

Under  $\text{H}_2\text{SO}_4$  treatment (3.2WBS), it was observed that the benzene ring and isolation of carbon and hydrogen from original WB structure remained. The intensities of C=O and C-O peaks were weaker compared to 3.2WBC[17, 75, 78]. Adsorption of symmetric and asymmetric stretching (S=O) of sulfonic group (-SO<sub>3</sub>H) was evident at  $1043$  and  $1080\text{ cm}^{-1}$ , confirming successful functionalization of sulfonic groups within 3.2WBS[80].

In case of  $\text{H}_3\text{PO}_4$  treatment (3.2WBP), the C-O stretching peak was weaker, like 3.2WBS. However, C=O peak remained unchanged compared to other samples. 3.2WBP treated with  $\text{H}_3\text{PO}_4$  exhibited grafting of functional groups in form of systematic vibrations of P-phosphate ester (P-O)[81] and polyphosphate (P-O-P) at wavenumber of  $1063\text{ cm}^{-1}$ [46, 72]. Additionally, C=C and C-H were detected at wavenumbers of  $1615$  and  $876\text{ cm}^{-1}$ , like biochar.

Furthermore, stretching vibrations around  $2358\text{ cm}^{-1}$  in all samples, indicated the adsorption of CO<sub>2</sub> from the air[50].

Based on FTIR results, it can be concluded that pristine biochar originally possessed acidic functional groups on its surface. After acid treatment, functionalized biochar observed similar functional groups but showed variations in peak intensities and incorporation of new functional groups. Biochar treated with HCl did not introduce new acidic functional groups; instead, it exhibited an enhancement in carboxylic groups and conversion of some original functional groups into single-bond oxygen functional groups. In contrast, biochar treated with  $\text{H}_2\text{SO}_4$  and  $\text{H}_3\text{PO}_4$  could graft new acidic functional groups, such as sulfonic and phosphate groups.

Therefore, as confirmed by the results, the presence of these acidic functional groups such as carboxylic groups, sulfonic groups, and phosphate groups could be beneficial in donating protons to expedite fructose dehydration into 5-HMF.

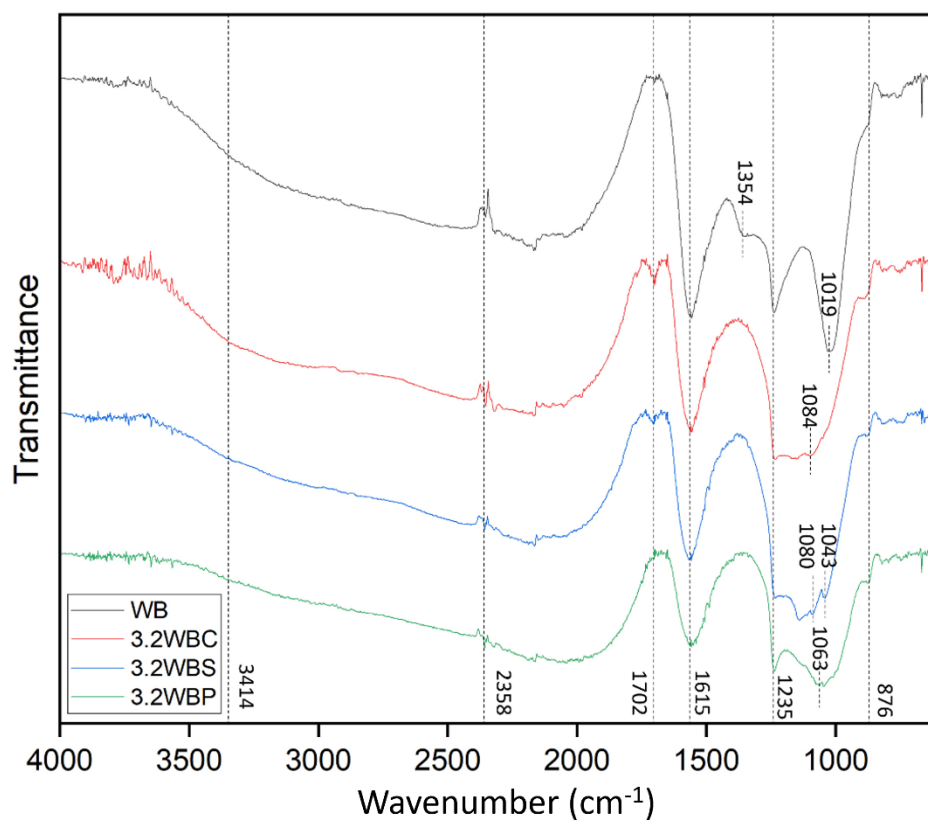


Figure 4-6 FTIR spectra of pristine and functionalized biochar

#### 4.2.5 Total acidity

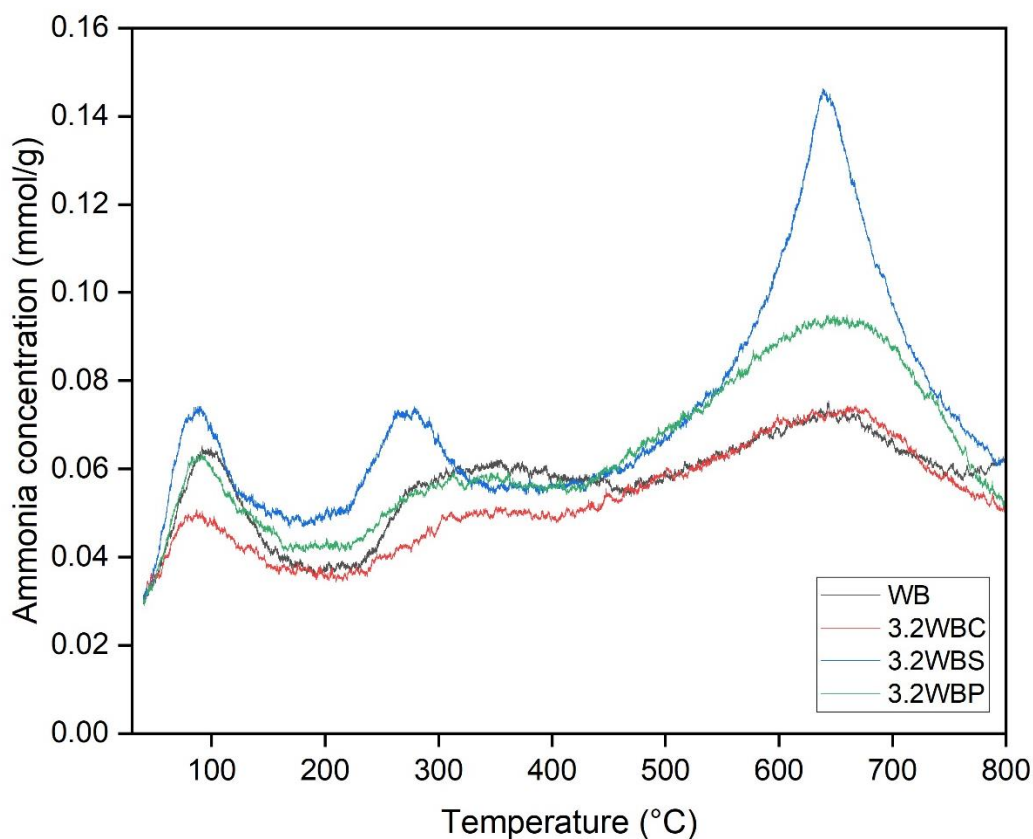


Figure 4-7 NH<sub>3</sub>-TPD results for pristine biochar and functionalized biochar.

NH<sub>3</sub>-TPD profiles, presented in Figure 4-7, were utilized to corroborate the presence of acidity alongside FTIR results. Total acidity was illustrated in Table 4-5. Distribution of various acid types was deduced from integration of ammonia concentration graphs. Dispersion of active acidic sites, as displayed in Figure 4-7, confirmed presence of acidic functional groups both before and after acid modification. Signal peaks observed below 100°C to 200°C indicated weak acid sites encompassing carboxylic groups. Peak in the range of around 200°C to 400°C represented moderate acid sites, including lactone, aldehyde, and sulfonic groups. Peak above 400°C to 950°C signify strong acid sites referred to as phenol and carbonyl groups, presented on surface[82]. Across samples, all exhibited three distinct peaks and intensities corresponding to weak, moderate, and strong acid sites.

Pristine biochar initially demonstrated three peaks, confirming presence of original acidic functional groups, including weak acid sites (0.59 mmol/g), moderate acid sites (0.59 mmol/g), and strong acid sites (1.49 mmol/g), totaling 2.67 mmol/g, consistent with FTIR results.

Treatment of pristine biochar with HCl (3.2WBC) resulted in an increase in total acidity to 2.98 mmol/g, owing to presence of three different peaks indicating weak (0.41 mmol/g), moderate (0.24 mmol/g), and strong acid sites (2.33 mmol/g). This increase in strong acid sites is attributed to enhancement of carbonyl groups and phenol (strong acid sites), akin to sharpened and broadened peak observed FTIR spectra of C=O and C-O after acid treatment. Increase in total acidity aligned with findings reported by Peiris et al.[48], which observed an enhancement of phenol and lactone, and reduction in carboxylic groups (weak acid sites) after HCl treatment.

After subjecting biochar to sulfuric acid treatment, total acidity of 3.2WBS increased to 4.56 mmol/g, closely resembling acidity reported for sulfonated graphene oxide (3.60 mmol/g) in prior study by Lawagon et al.[5]. Weak, moderate, and strong acid sites were observed, measuring 0.51, 0.36, and 3.69, respectively, indicating presence of carboxylic and phenol/carbonyl as weak and strong acid sites. Moderate sites were identified as sulfonic and lactone or aldehyde, consistent with findings reported by Umar et al.[82]. Presence of sulfonic groups resulted from grafting of sulfur trioxide fuming during sulfonation treatment, corroborated with CHNS/O analysis and FTIR.

In case of 3.2WBP, total acidity increased to 3.69 mmol/g after treatment with phosphoric acid. Enhanced total acidity was attributed to functionalization of phosphate groups on biochar surface, supported by FTIR spectra. This treatment exhibited peaks corresponding to weak, moderate, and strong acid sites, measuring 0.51, 0.26, and 2.96 mmol/g, respectively. Additionally, NH<sub>3</sub>-TPD profile indicated presence of P-containing groups with broad peak maximum temperature of 260°C, approximate to findings reported by Puziy et al[81]. These results contrasted previous observations of only weak and moderate acid sites in mesoporous carbon[47].

Results indicated that functionalized biochar demonstrated an increase in total acidity following acid treatment. Presence of acidic functional groups such as carboxylic, sulfonic, and phosphate groups, reported by FTIR spectra, suggested their potential behavior as acidic functional groups that can donate protons in fructose dehydration reaction.



Table 4-5 Acidity strength of WB and functionalized biochar

Samples	Total acidity (mmol/g)			
	Weak	Medium	Strong	Total
WB	0.59	0.59	1.49	2.67
3.2WBC	0.41	0.24	2.33	2.98
3.2WBS	0.51	0.36	3.69	4.56
3.2WBP	0.47	0.26	2.96	3.69

### 4.3 Catalytic performance of each acid-treated biochar

Because of different characteristics, each acid-treated biochar samples were anticipated to exhibit different catalytic performance. The catalytic performance, detailed in Table 4-6, revealed fructose conversion and product yields, including 5-HMF, levulinic acid, formic acid, furfural, and several by-products. Without catalyst, fructose conversion was merely 55.7%, resulting in a low 5-HMF yield of 36.5%. However, employing biochar solid catalysts significantly boosted fructose conversion to a range of 69.6% to 71.6%, indicating catalyst's role in accelerating 5-HMF formation by reducing activation energy.

Lima et al. reported that significance of various factors, including textural properties (mesoporous and microporous) and acidity strength (strength of acidity and total acidity) in influencing fructose dehydration. Their finding emphasize necessity of not singularly focus on single parameter (textural or acid properties) in dehydration optimization[56]. Their influence on 5-HMF production was examined individually for each characteristic as follows.

Pristine biochar, possessing large pore volumes and mesoporous pore width along with original acidic functional groups, provided fructose conversion of 71.4%. However, it yielded a meager 23.5% 5-HMF, with higher preference for by-product formation of 74.8%, such as humin or unidentified products. This instability in 5-HMF formation was attributed to various factors, including reactions involving water solvent

opening furan ring, acetal reactions between aldehyde group of 5-HMF and -OH groups of fructose, and grafting of hydroxyl groups of 5-HMF onto hexose moieties, as reported by Xu et al.[83]. Using water as a solvent led to observation of humin as by-product across all biochar catalysts. Presence of humin within biochar catalyst might result from reactions between -OH groups of alcohol on biochar (as confirmed by FTIR) and aldehyde group on 5-HMF. Additionally, 5-HMF might undergo etherification in the presence of catalyst and alcohol, forming a solid by-product of 5-EMF (solid humin), as reported by Guo et al.[84]. Darker appearance of liquid solution using WB catalyst further confirmed presence of high concentration of humin, indicating that main product derived was humin[46]. This observation was displayed in Figure 4-8.

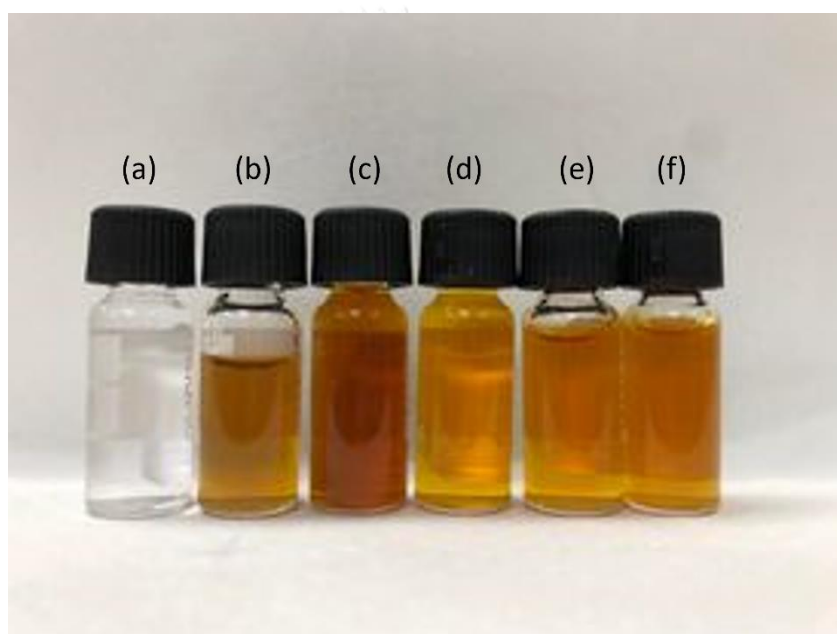


Figure 4-8 Liquid product from fructose dehydration using absence and presence biochar catalysts (a) fructose, (b) Blank, (C) WB, (d) 3.2WBC, (e) 3.2WBS, and (f) 3.2WBP

Comparing fructose conversions among functionalized biochar samples treated with equivalent concentrations, similar fructose conversions were observed (3.2WBC, 3.2WBS, and 3.2WBP at 71.6, 71.4, and 69.6%, respectively). Presence of acidic functional groups like carboxylic, sulfonic, and phosphoric groups, containing proton ions, could interact with -OH groups in fructose molecules, initiating removal of water molecules. Consequently, these acidic functional groups on biochar regained their acidic properties and became active, ultimately resulting in 5-HMF production after removal of three water molecules. Nonetheless, minor discrepancies in 5-HMF yields were noticed due to specific properties of biochar as follows.

3.2WBC sample exhibited 5-HMF yield of 43.7%, levulinic acid (5.2%), formic acid (33.9%), furfural (1.1%), and by-products (46.0%). Although possessing a total acidity of 2.97 mmol/g and carboxylic groups, it provided 5-HMF yields slightly lower than 3.2WBS samples. Presence of chloride ions resulting from HCl treatment of biochar might hinder 5-HMF formation, favoring furfural production[85]. Amount of chloride ions was confirmed using FESEM/EDX, as displayed in APPENDIX B. However, difference in furfural amounts between different biochar catalysts was negligible, differing only by 0.2%.

3.2WBS sample showed a slight improvement in 5-HMF yield compared to 3.2WBC, achieving a 5-HMF yield of 45%, attributed to presence of sulfonic groups, as reported by Li et al[85]. Notably, when compared to sulfonated carbon nanoparticle catalyst derived from eucalyptus oil, catalyst achieved similar fructose conversion rates of 84.0% and yielded 51.6% in 5-HMF yield production[16]. However, like 3.2WBC, it also generated by-products such as levulinic acid (3.0%), formic acid (5.4%), furfural (0.9%), and by-products (45.8%).

Treatment with phosphoric acid (3.2WBP) resulted in fructose conversion and 5-HMF yield of 69.6%, and 42.0%, respectively. Moreover, it produced formic acid, levulinic acid, furfural, and by-products, yielding 3.3, 4.4, 1.0, and 49.3%, respectively. Notably, generation of by-products was higher in case of 3.2WBC and 3.2WBS compared to 3.2WBP. This increase in by-product in 3.2WBP might be due to its smaller pore volume, making it challenging to remove 5-HMF from pore sites, thus leading to side reactions with other acid sites. Presence of phosphate groups, displayed in *ผลิตภัณฑ์: ไม่พบแหล่งการอ้างอิง*, facilitated incorporation of hydroxyl groups with P-OH, providing a proton for fructose dehydration. Phosphate biochar (3.2WBP) notably improved 5-HMF selectivity to 62.9%, a much higher value compared to selectivity provided by phosphorylated xerogel, which was only 39.2% [86].

Comparing yield of 5-HMF among various functionalized biochar samples with equivalent acid concentrations demonstrated similar results. However, presence of specific functional groups had a slight impact on 5-HMF yield, as reported with prior research emphasizing pivotal role of such functional groups in 5-HMF production, as reported by Villa et al.[87]. In this study, sulfur functional groups presented the highest selectivity of 62.9%, followed by carboxylic functional groups at 61.2% and phosphorous functional groups at 60.3%.

Considering significance of grafting sulfonic groups and successful 5-HMF selectivity observed in 3.2WBS sample, further investigation will focus on biochar treated with sulfuric acid to examine concentration effect in subsequent parts.

Table 4-6 Performance tests of pristine biochar and pristine biochar

Samples	No catalyst	WB	3.2WBC	3.2WBS	3.2WBP
Fructose conversion (%)	55.7±1.3	71.4±0.3	71.6±0.2	71.4±0.0	69.6±0.0
5-HMF yield (%)	36.5±1.6	23.5±0.1	43.7±0.0	45.0±0.0	42.0±0.1
Formic acid yield (%)	2.8±0.8	1.4±0.8	5.2±0.9	5.4±0.5	4.4±0.2
Levulinic acid yield (%)	2.0±0.0	0±0.0	3.9±2.6	3.0±0.8	3.3±0.1
Furfural yield (%)	0.8±0.1	0.4±0.1	1.1±0.2	0.9±0.1	1.0±0.0
Other products such as humin, unknown (%)	57.9±2.4	74.8±1.0	46.0±1.9	45.8±1.5	49.3±0.2
5-HMF selectivity (%)	65.4±1.3	32.9±0.1	61.2±0.1	62.9±0.1	60.3±0.0

#### 4.4 Effect of sulfuric acid concentration on characteristics of sulfonated biochar

Upon results of Part 4.2 (Influence of types of acids), sulfuric acid treatment showed potential for enhancing biochar properties. Samples were modified with sulfuric acid and referred to as sulfonated biochar. However, concentrations of sulfuric solution could significantly influence biochar properties, which were investigated in this section with concentrations of 1.6, 3.2, and 4.8 N, as detailed below. Sulfonated biochar were determined as 1.6WBS, 3.2WBS, and 4.8WBS, corresponding to various concentrations.

##### 4.4.1 Chemical compositions, Yields, and Ash

Different concentrations vary in terms of number of proton ions and sulfur groups. In this case, the highest amounts of protons and sulfur groups were obtained by 4.8N sulfuric solution (4.8WBS), followed by 3.2N and 1.6N solutions, respectively. Based on results presented in Table 4-7, masses of 1.6WBS, 3.2WBS, and 4.8WBS after acid treatment were found to be 60.6, 60.1, and 53.9%, respectively. Protons from acid solution contributed to devastation of biochar structure and removal of impurities, leading to reduction in biochar mass.

Comparing sulfonated samples, percentages of carbon, hydrogen, and nitrogen showed negligible changes. Increase in nitrogen contents is attributed to low volatilization of nitrogen during sulfonation[49]. In contrast, sulfur compounds in 1.6WBS, 3.2WBS, and 4.8WBS significantly increased to 1.4, 1.9, and 2.2, respectively, as a result of grafting of sulfonic groups on biochar surface[88]. This implied that higher concentrations of sulfuric acid can enhance sulfonation, a fact further confirmed using FTIR analysis. Furthermore, ash content decreased from 3.3% to 2.6% as sulfuric solution increased.

Table 4-7 Product yields, ash, and chemical contents in sulfonated biochar

Samples	Product yield (%)	Ash (%)	Percentage of elements (%)				
			C	H	N	S	O <sup>b</sup>
1.6WBS	60.6±2.4 <sup>a</sup>	3.3	72.0	1.7	1.5	1.4	23.4
3.2WBS	60.1±1.8 <sup>a</sup>	2.6	71.8	1.7	1.7	1.9	22.9
4.8WBS	53.9±2.2 <sup>a</sup>	2.7	69.1	1.8	4.6	2.2	22.3

a: amount of activated biochar obtained after chemical modification.

b: by difference

#### 4.4.2 Morphology

Morphology of sulfonated biochar revealed large amount of porosity after acid treatment, as displayed in Figure 4-9(a), (c), and (e). The porous structure was observed, thanks to cleaning effect of acid solution, consequently unblocking the pore channel, as illustrated in Figure 4-9(b), (d), and (f)[68].

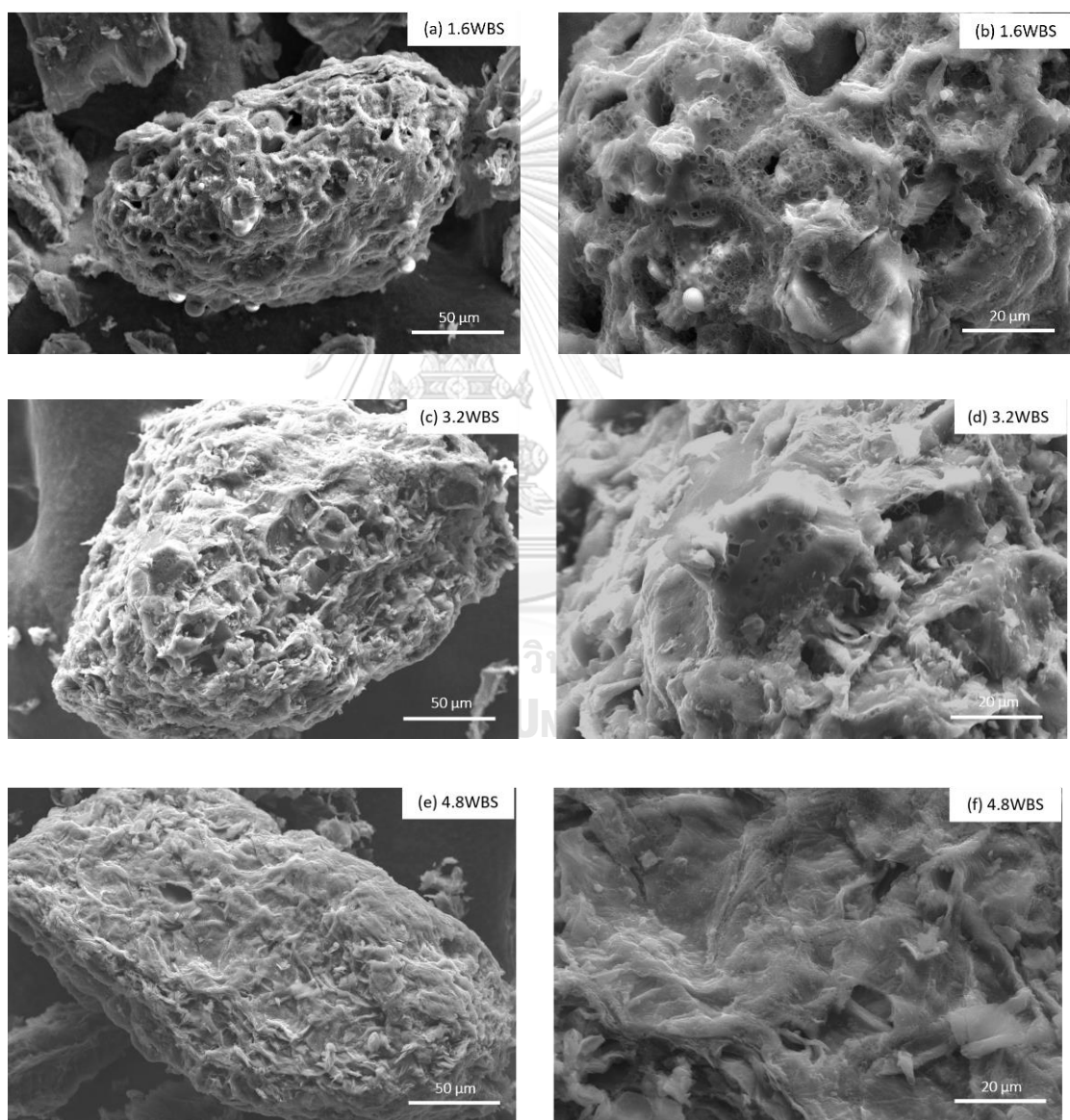


Figure 4-9 FESEM images of sulfonated biochar at magnifications of 1,500x (a, c, e) and 5,000x (b, d, f)

#### 4.4.3 Porous properties

BET isotherms of sulfonated biochar were shown in Figure 4-10. It exhibited hysteresis loop Type IV isotherms at relative pressure in range of 0.4 to 0.1, indicating the presence of mesopores. Furthermore, quantity of adsorbed significantly increased at low relative pressure, implying the existence of micropore structure.

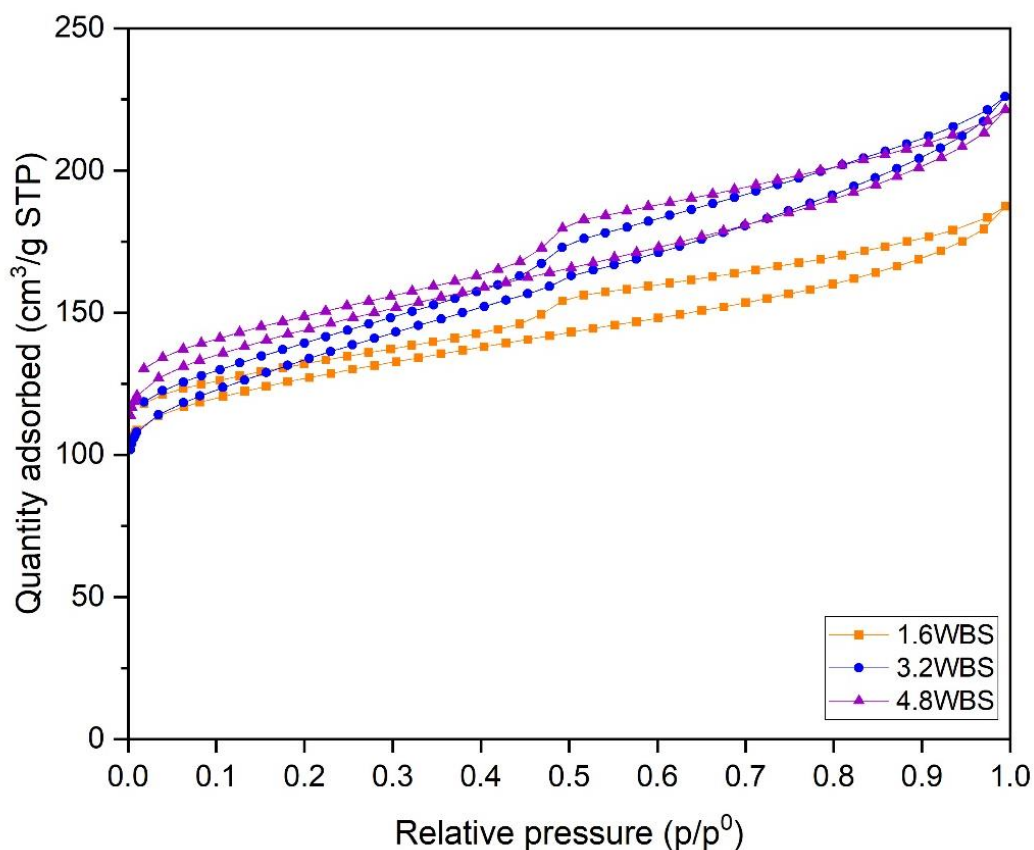


Figure 4-10 BET isotherms of sulfonated biochar

Specific surface, pore volume, and pore width of sulfonated samples were summarized in Figure 4-10.  $S_{BET}$  of 1.6WBS, 3.2WBS, and 4.8WBS was 405.6, 438.7, and 463.8  $m^2/g$ , respectively.  $S_{BET}$  tended to increase as acid solution concentration increased, as the higher amount of proton ions could disrupt biochar structure and generate micropores[71].

Increase in concentration from 1.6 N to 3.2 N resulted in tendency for pore volume to rise from 0.13  $cm^3/g$  to 0.20  $cm^3/g$ , indicating the emergence of newly generated micropores. With a further increase in concentration to 4.8 N, pore volume slightly decreased to 0.18  $cm^3/g$ . This decrease could be attributed to excessive sulfur groups leading to clogging of the pores. Regarding pore size, all of samples exhibited similar pore sizes in range of 4.3-4.4 nm.

Therefore, as the concentrations of sulfuric increased, there was minimal impact on textural properties regarding pore volume and pore width. However, a slight increase in specific surface area was observed as a concentration increased.

Table 4-8 Physical properties of sulfonated biochar

Sample	$S_{BET}$ (m <sup>2</sup> /g)	$V_p$ (cm <sup>3</sup> /g)	$D_{avg}$ (nm)
1.6WBS	405.6	0.13	4.4
3.2WBS	438.7	0.20	4.3
4.8WBS	463.8	0.18	4.3

#### 4.4.4 Surface functional groups

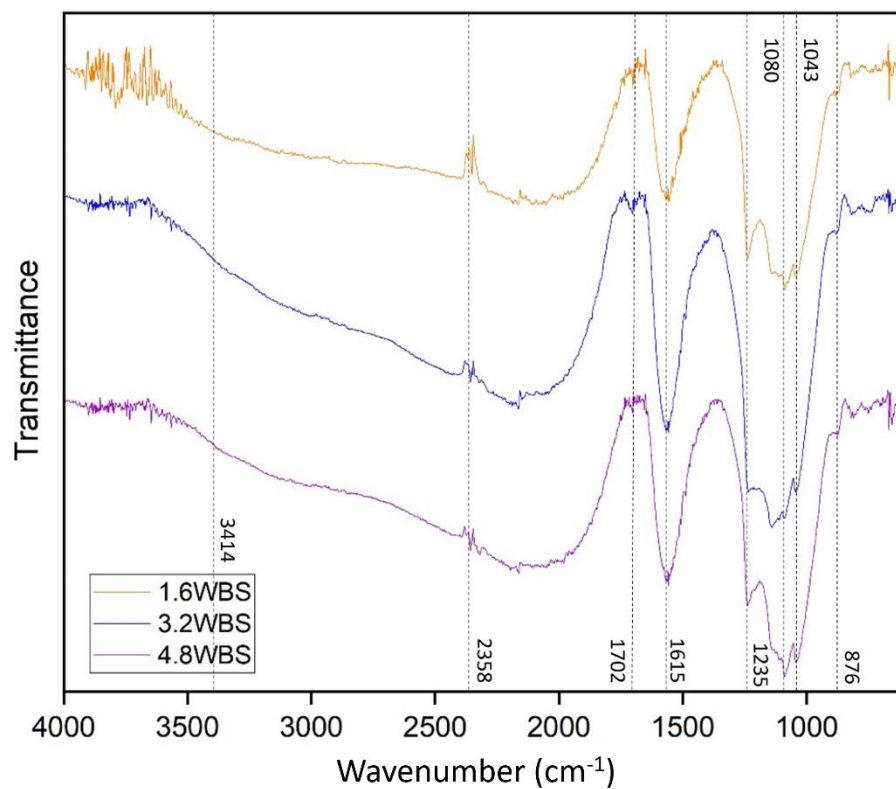


Figure 4-11 FTIR spectra of sulfonated biochar



FTIR spectra of sulfonated biochar were depicted in Figure 4-11. For 1.6WBS sample, presence of aliphatic bending groups (C-H) in biochar structure was observed at  $876\text{ cm}^{-1}$ [48]. Wavelength at  $1615\text{ cm}^{-1}$  indicated condensation of C=C aromatic structures[48, 73]. Stretching vibrations of carboxylic, and phenol groups were detected at bands around  $1702\text{ cm}^{-1}$  and  $1235\text{ cm}^{-1}$ , respectively. Additionally, a weaker peak of sulfonic group (S=O) stretching vibration appeared around  $1043\text{ cm}^{-1}$  and  $1080\text{ cm}^{-1}$  due to lower sulfuric concentration.

In case of 3.2WBS, original lignocellulosic structures, such as aliphatic, benzene ring structures, and phenols, appeared similarly to FTIR spectra of pristine biochar and 1.6WBS. Peaks of carboxylic, and sulfonic groups ( $1702\text{ cm}^{-1}$ ,  $1043\text{ cm}^{-1}$  and  $1080\text{ cm}^{-1}$ ) exhibited increased intensities due to stronger acid concentration increasing from 1.6 N to 3.2 N.

For sulfonated biochar treated with concentration of 4.8 N (4.8WBS), old functional groups such as C-H, C=C, C=O, and C-O were observed at wavelengths of  $876\text{ cm}^{-1}$ ,  $1558\text{ cm}^{-1}$ ,  $1702\text{ cm}^{-1}$  and  $1235\text{ cm}^{-1}$ , respectively. A strong peak of sulfonic groups around  $1037\text{ cm}^{-1}$  aligned with an increase in sulfuric acid concentration from 3.2 N to 4.8 N.

Presence of sulfonic groups in all samples confirmed functionalized sulfonic groups on biochar, consistent with CHNS/O analysis. Increase in sulfuric concentration influenced number of sulfonic groups and total acidity, as demonstrated by  $\text{NH}_3$ -TPD results. Moreover, presence of sulfonic groups may affect formation of 5-HMF, as reported in a previous study[16].

#### 4.4.5 Total acidity strength

Acidity strength of sulfonated biochar was confirmed through  $\text{NH}_3$ -TPD results, as displayed in Figure 4-12 and summarized in Table 4-9. In Figure 4-12, observation of 1.6WBS, 3.2WBS, and 4.8WBS revealed distinct intensity peaks corresponding to weak (below  $200^\circ\text{C}$ ), medium ( $200$ - $400^\circ\text{C}$ ), and strong ( $400$ - $950^\circ\text{C}$ ) acidity ranges[82]. Broadened peaks observed in all sulfonated biochar around  $200^\circ\text{C}$  to  $400^\circ\text{C}$  confirmed presence of sulfonic group ( $-\text{HSO}_3$ ), indicating their onset of thermal decomposition[89, 90]. Total acidity of sulfonated biochar, as revealed by  $\text{NH}_3$ -TPD profiles, as detailed in Table 4-9.

Upon comparing various concentrations, transition from 1.6 N to 3.2 N exhibited an increase in total acidity from 3.88 to 4.56 mmol/g with rising concentration, attributed to incorporation of sulfonic groups, consistent with CHNS/O results[49]. However, with increase in concentration from 3.2 N to 4.8 N, there was slight decrease in total acidity of weak and strong acid sites from 4.56 to 4.31 mmol/g.

The decrease in total acidity could be due to the higher acid strength solution corroding original acidic functional groups on biochar surface. Moreover, according to Gong et al., pyrolysis treatment affected to biochar structure, it remained a main of carbon benzene ring, with fewer functional groups at the edge of benzene rings. Sulfonic-containing groups may exhibit a preference for bonding with functional groups rather than with benzene rings. Consequently, with fewer functional groups presented in pristine biochar, the capacity for grafting new functional groups became limited. Any excess non-incorporated acidic groups would be removed by water[73].

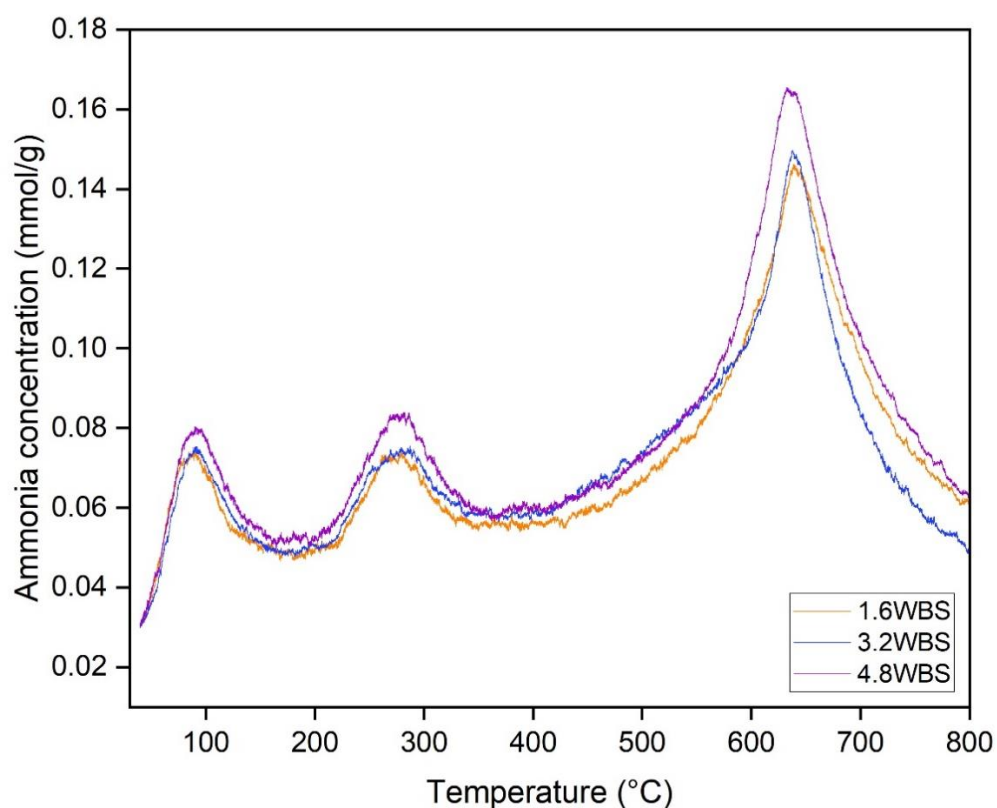


Figure 4-12 NH<sub>3</sub>-TPD profile of sulfonated biochar

Table 4-9 Total acidity strength of sulfonated biochar

Samples	Acidity (mmol/g)			
	Weak	Medium	Strong	Total

1.6WBS	0.42	0.34	3.12	3.88
3.2WBS	0.51	0.36	3.69	4.56
4.8WBS	0.46	0.39	3.46	4.31

#### 4.5 Catalytic performance of sulfonated biochar

Performance of sulfonated biochar catalyst in fructose dehydration was detailed in Table 4-10. Sulfonated biochar, treated with various concentrations, caused fructose conversions ranging from 71.0 % to 72.3%. 5-HMF yields of 1.6WBS, 3.2WBS, and 4.8WBS were 42.0%, 45.0%, and 46.0%, respectively. Additionally, 5-HMF could undergo further reactions, resulting in production of by-products such as levulinic acid, formic acid, furfural, and humin.

Sulfonated biochar with concentration of 1.6 N, exhibiting the lowest pore volume and total acidity, resulted in the lowest 5-HMF yield (42%). However, increasing concentration to 3.2 N enhanced the 5-HMF yields to 45% due to higher pore volume, facilitating the easier diffusion of 5-HMF out of catalyst pores. This increase in sulfonic groups led to enhancement of reactive sites and catalytic activity[49]. In contrast, as sulfuric concentration was raised from 3.2 N to 4.8 N, there was only slight enhancement, resulting in a mere 1% increase in 5-HMF yield. This minor increase could be attributed to excess sulfate ions remaining in biochar pore. These ions reacted with water rather than the 5-HMF molecule, stabilizing 5-HMF molecule[91].

Moreover, selectivity of 5-HMF increased with augmentation of acid concentration, rising from 58.4% to 63.5%. Nevertheless, when considering achieved 5-HMF yields across various acid concentrations, 4.8N concentration stood out as remarkable sulfonated biochar candidate.

Table 4-10 Catalytic performance of sulfonated biochar

Samples	1.6WBS	3.2WBS	4.8WBS
Fructose conversion (%)	71.9±0.1	71.4±0.0	72.3±1.7

5-HMF yield (%)	42.0±0.1	45.0±0.0	46.0±0.3
Formic acid yield (%)	4.9±0.2	5.4±0.5	5.3±1.5
Levulinic acid yield (%)	3.4±2.1	3.0±0.8	4.6±2.1
Furfural yield (%)	1.0±0.1	0.9±0.1	0.8±0.1
Other products such as humin, unknown (%)	48.7±2.6	45.8±1.5	43.3±0.3
5-HMF selectivity (%)	58.4±0.0	62.9±0.1	63.5±0.0

Activity of functionalized biochar in terms of fructose conversion and 5-HMF selectivity was compared to other types of solid catalysts, as displayed in Table 4-11. Synthesis of functionalized biochar derived from watermelon rind, through pyrolysis and hydrothermal treatment, demonstrated remarkable performance as heterogeneous catalyst in converting fructose into 5-HMF.

Table 4-11 Fructose conversion into 5-HMF using various catalyst.

Samples	Feedstock	Type and concentration of acid treatment	Temperature (°C)	Time (mins)	Solvent	Fructose conversion (%)	5-HMF selectivity (%)	Ref.
CX_P	Carbon gel	24 N of H <sub>3</sub> PO <sub>4</sub>	180	120	DI	75.4	39	Eblagon et al. (2023)[86]
PAB2-600	Pinewood sawdust	42 N of H <sub>3</sub> PO <sub>4</sub>	160	20	DMSO	/	56	Cao et al. (2018)[46]
40%-H <sub>3</sub> PO <sub>4</sub> /AC	Activated carbon	20 N of H <sub>3</sub> PO <sub>4</sub>	180	20	DMSO	100	88	Ferreira et al. (2023)[92]
Sulfonated biochar-30	Wood waste	6 N of H <sub>2</sub> SO <sub>4</sub>	180	20	DI	/	59	Xiong et al.(2018)[10]
Sulfonated magnetic carbon	Eucalyptus oil and Ferrocene	36 N of H <sub>2</sub> SO <sub>4</sub>	180	30	DI	84	60.7	Giang et al.(2021)[16]
CS-2	Glucose	36 N of H <sub>2</sub> SO <sub>4</sub>	125	30	DMSO	86	72	Zhao et al. (2016)[93]
WB	Watermelon rind	-	160	90	DI	71	33	This work
3.2WBC		3.2 N of HCl				71	61	
3.2WBP		3.2 N of H <sub>3</sub> PO <sub>4</sub>				69	60	
1.6WBS		1.6 N of H <sub>2</sub> SO <sub>4</sub>				71	58	

3.2WBS		3.2 N of $\text{H}_2\text{SO}_4$				71	63	
4.8WBS		4.8 N of $\text{H}_2\text{SO}_4$				72	64	



## CHAPTER 5

### CONCLUSIONS AND RECOMMENDATIONS

This chapter consists of four parts. The first three parts concluded the process, covering the preparation of dried watermelon rind biochar, synthesis of functionalized biochar, and the impact of various types and concentrations of acids on catalytic performance test. The final part focused on recommendations for the future works as follows.

#### 5.1 Preparation of pristine biochar from dried watermelon rind

After pyrolyzing dried watermelon rind, it produced 35.2% watermelon rind biochar due to thermal decomposition of lignocellulosic contents. The decomposition decreased the percentage of hydrogen, nitrogen, and oxygen, resulting in increased carbon fraction. Furthermore, specific surface area and pore volume of watermelon rind biochar were increased, measuring  $394.3 \text{ m}^2/\text{g}$ , and  $0.45 \text{ cm}^3/\text{g}$ , respectively.

#### 5.2 Effect of acid treatment on characteristics of acid-treated biochar

Type of acid utilized with equivalent concentration for biochar modification could impact the physiochemical properties of biochar, including specific surface area, chemical compositions, surface functional groups, and acidity strength. Acid modification typically augments specific surface area by initiating acid corrosion, removing fine particles from original pores and creating micropores. However, this process may slightly reduce pore volume and width due to pore blockage by anion-containing groups.

Pristine biochar treated with HCl, the most potent acid solution, exhibited the highest specific surface area, pore volume, and pore width, measuring  $497 \text{ m}^2/\text{g}$ ,  $0.41 \text{ cm}^3/\text{g}$ , and  $3.3 \text{ nm}$ , respectively. Although pristine biochar may possess original acidic functional groups like carboxylic, HCl treatment does not introduce new functional groups. Conversely,  $\text{H}_2\text{SO}_4$  and  $\text{H}_3\text{PO}_4$  treatment could embed new functional groups containing sulfur and phosphorous.

Furthermore, acid modification could enhance total acidity in biochar. Among samples, 3.2WBS exhibited the highest total acidity strength of  $4.5 \text{ mmol/g}$ , while 3.2WBP and 3.2WBC showed lower total acidity at  $3.7$  and  $2.9 \text{ mmol/g}$ , respectively.

Biochar catalysts significantly increased fructose conversion from  $55.8\%$  to  $71.6\%$ . Treatment with sulfuric acid achieved a fructose conversion of  $71.4\%$  and improved 5-HMF yield to  $45\%$  by grafting of sulfonic groups on its surface. As a result,

sulfuric acid appeared promising for further investigation, particularly to study effect of various concentrations in the next part.

### **5.3 Effect of sulfuric concentration on characteristics of sulfonated biochar**

Properties of sulfonated biochar exhibited slight alternations with increasing concentration, affecting specific surface area, chemical elements, surface functional groups, and acidity strength. As concentration of sulfuric acid solution rose, sulfonated biochar manifested higher specific surface area and pore volume. Notably, biochar treated with 4.8N displayed the highest specific surface area (464 m<sup>2</sup>/g) and pore volume (0.33 cm<sup>3</sup>/g) among variants.

Comparatively, all sulfonated biochar samples, particularly those treated with concentrations of 4.8N, showed a more pronounced peak of sulfonic groups grafted onto biochar surface, in line with the highest sulfur contents of 2.2% observed among samples. Total acidity measurements for 1.6WBS, 3.2WBS, and 4.8WBS were 3.88, 4.56, and 4.31 mmol/g, respectively.

Remarkably, among these samples, sulfonated biochar (4.8WBS), treated with a 4.8 N acid solution, demonstrated outstanding catalytic performance in fructose dehydration, achieving a conversion rate of 72.3%, 5-HMF yield of 46%, and 5-HMF selectivity of 63.5%.

Thus, functionalized biochar, prepared through a combination of pyrolysis and hydrothermal treatment, serves as an effective heterogeneous catalyst to produce 5-HMF.

### **5.4 Remaining issues and Recommendations**

5.4.1 This study controlled only type of feedstock, namely watermelon rind. However, other biomass source available in Thailand, such as sugarcane, water hyacinth, or rice grass, could potentially serve as viable alternatives in preparing catalysts.

5.4.2 This finding revealed that an increase in pyrolysis temperature significantly affected biochar properties, such as specific surface area and functional groups. From an economic perspective, utilizing lower temperatures in biochar preparation could potentially reduce costs involved in generating acidic biochar catalysts.

5.4.3 This work is limited in terms of purifying 5-HMF from other products. There is an interest in further developing this process.

5.4.4 Due to time constraints, catalyst regeneration testing was not conducted in this work. Further studies are recommended to confirm the reusability of catalyst.



## REFERENCES



จุฬาลงกรณ์มหาวิทยาลัย  
**CHULALONGKORN UNIVERSITY**

1. Chen, H., 5 - Lignocellulose biorefinery product engineering, in Lignocellulose Biorefinery Engineering, H. Chen, Editor. 2015, Woodhead Publishing. p. 125-165.
2. Yang, H., et al., In-Depth Investigation of Biomass Pyrolysis Based on Three Major Components: Hemicellulose, Cellulose and Lignin. *Energy & Fuels*, 2006. 20(1): p. 388-393.
3. Kruger, J.S., et al., Elucidating the Roles of Zeolite H-BEA in Aqueous-Phase Fructose Dehydration and HMF Rehydration. *ACS Catalysis*, 2013. 3(6): p. 1279-1291.
4. Yu, I.K.M., et al., Catalytic valorization of starch-rich food waste into hydroxymethylfurfural (HMF): Controlling relative kinetics for high productivity. *Bioresource Technology*, 2017. 237: p. 222-230.
5. Lawagon, C.P., et al., Sulfonated graphene oxide from petrochemical waste oil for efficient conversion of fructose into levulinic acid. *Catalysis Today*, 2021. 375: p. 197-203.
6. Wang, H., et al., Recent advances in catalytic conversion of biomass to 5-hydroxymethylfurfural and 2, 5-dimethylfuran. *Renewable and Sustainable Energy Reviews*, 2019. 103: p. 227-247.
7. Boisen, A., et al., Process integration for the conversion of glucose to 2,5-furandicarboxylic acid. *Chemical Engineering Research and Design*, 2009. 87(9): p. 1318-1327.
8. Karimi, S., et al., Catalytic dehydration of fructose into 5-hydroxymethylfurfural by propyl sulfonic acid functionalized magnetic graphene oxide nanocomposite. *Renewable Energy*, 2021. 180: p. 132-139.
9. Deshan, A.D.K., et al., Structural features of cotton gin trash derived carbon material as a catalyst for the dehydration of fructose to 5-hydroxymethylfurfural. *Fuel*, 2021. 306: p. 121670.
10. Xiong, X., et al., Sulfonated biochar as acid catalyst for sugar hydrolysis and dehydration. *Catalysis Today*, 2018. 314: p. 52-61.
11. Lee, Y.-Y. and K.C.W. Wu, Conversion and kinetics study of fructose-to-5-hydroxymethylfurfural (HMF) using sulfonic and ionic liquid groups bi-functionalized mesoporous silica nanoparticles as recyclable solid catalysts in DMSO systems. *Physical Chemistry Chemical Physics*, 2012. 14(40): p. 13914-13917.
12. Dibenedetto, A., et al., Conversion of fructose into 5-HMF: a study on the behaviour of heterogeneous cerium-based catalysts and their stability in aqueous media under mild conditions. *RSC Advances*, 2015. 5(34): p. 26941-26948.
13. Qiu, G., et al., Tin-modified ionic liquid polymer: A novel and efficient catalyst for synthesis of 5-hydroxymethylfurfural from glucose. *Fuel*, 2020. 268: p. 117136.
14. Ramírez Bocanegra, N., et al., Catalytic conversion of 5-hydroxymethylfurfural (5-HMF) over Pd-Ru/FAU zeolite catalysts. *Catalysis Today*, 2021. 360: p. 2-11.
15. Tempelman, C.H.L., et al., Processing of agricultural apple fruit waste into sugar rich feedstocks for the catalytic production of 5-HMF over a Sn Amberlyst-15 resin catalyst. *Journal of Industrial and Engineering Chemistry*, 2021. 99: p. 443-448.
16. Le, G.T.T., et al., Sulfonated magnetic carbon nanoparticles from eucalyptus oil as a green and sustainable catalyst for converting fructose to 5-HMF. *Catalysis Communications*, 2021. 149: p. 106229.

17. Guo, H., et al., Weak-acid biochar catalyst prepared from mechanochemically-activated biomass and humic acid for production of 5-hydroxymethylfurfural. *Biochar*, 2022. 4(1): p. 42.
18. Tag, A.T., et al., Effects of feedstock type and pyrolysis temperature on potential applications of biochar. *Journal of Analytical and Applied Pyrolysis*, 2016. 120: p. 200-206.
19. Saffari, N., et al., Biochar type and pyrolysis temperature effects on soil quality indicators and structural stability. *Journal of Environmental Management*, 2020. 261: p. 110190.
20. Dowaki, T., H. Guo, and R.L. Smith, Lignin-derived biochar solid acid catalyst for fructose conversion into 5-ethoxymethylfurfural. *Renewable Energy*, 2022. 199: p. 1534-1542.
21. Ahamad, S., et al., Recent trends in preprocessing and extraction of watermelon rind extract: A comprehensive review. *Journal of Food Processing and Preservation*, 2022. 46(7): p. e16711.
22. Thangavel, R., et al., High-energy green supercapacitor driven by ionic liquid electrolytes as an ultra-high stable next-generation energy storage device. *Journal of Power Sources*, 2018. 383: p. 102-109.
23. Rosatella, A.A., et al., 5-Hydroxymethylfurfural (HMF) as a building block platform: Biological properties, synthesis and synthetic applications. *Green Chemistry*, 2011. 13(4): p. 754-793.
24. Kuster, B.F.M., 5-Hydroxymethylfurfural (HMF). A Review Focussing on its Manufacture. *Starch - Stärke*, 1990. 42(8): p. 314-321.
25. Lee, H.S. and S. Nagy, RELATIVE REACTIVITIES of SUGARS IN the FORMATION of 5-HYDROXYMETHYLFURFURAL IN SUGAR-CATALYST MODEL SYSTEMS1. *Journal of Food Processing and Preservation*, 1990. 14(3): p. 171-178.
26. Antal, M.J., W.S.L. Mok, and G.N. Richards, Mechanism of formation of 5-(hydroxymethyl)-2-furaldehyde from d-fructose and sucrose. *Carbohydrate Research*, 1990. 199(1): p. 91-109.
27. Aida, T.M., et al., Reactions of d-fructose in water at temperatures up to 400°C and pressures up to 100MPa. *The Journal of Supercritical Fluids*, 2007. 42(1): p. 110-119.
28. Shaikh, M., et al., Graphene oxide as a sustainable metal and solvent free catalyst for dehydration of fructose to 5-HMF: A new and green protocol. *Catalysis Communications*, 2018. 106: p. 64-67.
29. Tao, F., H. Song, and L. Chou, Dehydration of fructose into 5-hydroxymethylfurfural in acidic ionic liquids. *RSC Advances*, 2011. 1(4): p. 672-676.
30. De Souza, R.L., et al. 5-Hydroxymethylfurfural (5-HMF) Production from Hexoses: Limits of Heterogeneous Catalysis in Hydrothermal Conditions and Potential of Concentrated Aqueous Organic Acids as Reactive Solvent System. *Challenges*, 2012. 3, 212-232 DOI: 10.3390/challe3020212.
31. Sajid, M., et al., Organic acid catalyzed production of platform chemical 5-hydroxymethylfurfural from fructose: Process comparison and evaluation based on kinetic modeling. *Arabian Journal of Chemistry*, 2020. 13(10): p. 7430-7444.

32. Hansen, T.S., J.M. Woodley, and A. Riisager, Efficient microwave-assisted synthesis of 5-hydroxymethylfurfural from concentrated aqueous fructose. *Carbohydrate Research*, 2009. 344(18): p. 2568-2572.
33. Fachri, B.A., et al., Experimental and Kinetic Modeling Studies on the Sulfuric Acid Catalyzed Conversion of d-Fructose to 5-Hydroxymethylfurfural and Levulinic Acid in Water. *ACS Sustainable Chemistry & Engineering*, 2015. 3(12): p. 3024-3034.
34. Wrigstedt, P., J. Keskiäli, and T. Repo, Microwave-enhanced aqueous biphasic dehydration of carbohydrates to 5-hydroxymethylfurfural. *RSC Advances*, 2016. 6(23): p. 18973-18979.
35. Asghari, F.S. and H. Yoshida, Kinetics of the Decomposition of Fructose Catalyzed by Hydrochloric Acid in Subcritical Water: Formation of 5-Hydroxymethylfurfural, Levulinic, and Formic Acids. *Industrial & Engineering Chemistry Research*, 2007. 46(23): p. 7703-7710.
36. Sánchez, J., et al., Chapter Two - Biomass Resources, in *The Role of Bioenergy in the Bioeconomy*, C. Lago, N. Caldés, and Y. Lechón, Editors. 2019, Academic Press. p. 25-111.
37. Neglo, D., et al., Comparative antioxidant and antimicrobial activities of the peels, rind, pulp and seeds of watermelon (*Citrullus lanatus*) fruit. *Scientific African*, 2021. 11: p. e00582.
38. Reddy, N.A., R. Lakshmipathy, and N.C. Sarada, Application of *Citrullus lanatus* rind as biosorbent for removal of trivalent chromium from aqueous solution. *Alexandria Engineering Journal*, 2014. 53(4): p. 969-975.
39. Lakshmipathy, R. and N.C. Sarada, Application of watermelon rind as sorbent for removal of nickel and cobalt from aqueous solution. *International Journal of Mineral Processing*, 2013. 122: p. 63-65.
40. Sajjadi, B., et al., Chemical activation of biochar for energy and environmental applications: A comprehensive review. *Reviews in Chemical Engineering*, 2018. 35.
41. Hagen, M.v.d. and J. Järnberg, Sulphuric, hydrochloric, nitric and phosphoric acids. 2009, The Nordic Expert Group for Criteria Documentation of Health Risk from Chemicals.
42. Mei, Y., et al., The dissociation mechanism and thermodynamic properties of HCl(aq) in hydrothermal fluids (to 700 °C, 60 kbar) by ab initio molecular dynamics simulations. *Geochimica et Cosmochimica Acta*, 2018. 226: p. 84-106.
43. Margarella, A.M., et al., Dissociation of Sulfuric Acid in Aqueous Solution: Determination of the Photoelectron Spectral Fingerprints of H<sub>2</sub>SO<sub>4</sub>, HSO<sub>4</sub><sup>-</sup>, and SO<sub>4</sub><sup>2-</sup> in Water. *The Journal of Physical Chemistry C*, 2013. 117(16): p. 8131-8137.
44. Gouveia, D., A. Bressiani, and J. Bressiani, Phosphoric Acid Rate Addition Effect in the Hydroxyapatite Synthesis by Neutralization Method. *Materials Science Forum - MATER SCI FORUM*, 2006. 530-531: p. 593-598.
45. Hao, H., et al. Synthesis of Sulfonated Carbon from Discarded Masks for Effective Production of 5-Hydroxymethylfurfural. *Catalysts*, 2022. 12, DOI: 10.3390/catal12121567.
46. Cao, L., et al., Phosphoric acid-activated wood biochar for catalytic conversion of starch-rich food waste into glucose and 5-hydroxymethylfurfural. *Bioresource Technology*, 2018. 267: p. 242-248.

47. Wang, L., et al., Phosphorylated ordered mesoporous carbon as a novel solid acid catalyst for the esterification of oleic acid. *Catalysis Communications*, 2014. 56: p. 164-167.
48. Peiris, C., et al., The influence of three acid modifications on the physicochemical characteristics of tea-waste biochar pyrolyzed at different temperatures: a comparative study. *RSC Advances*, 2019. 9(31): p. 17612-17622.
49. Mengstie, M.A. and N.G. Habtu, Synthesis and Characterization of 5-Hydroxymethylfurfural from Corncob Using Solid Sulfonated Carbon Catalyst. *International Journal of Chemical Engineering*, 2020. 2020: p. 8886361.
50. Tomer, R. and P. Biswas, Dehydration of glucose/fructose to 5-hydroxymethylfurfural (5-HMF) over an easily recyclable sulfated titania (SO<sub>4</sub><sup>2-</sup>/TiO<sub>2</sub>) catalyst. *New Journal of Chemistry*, 2020. 44(47): p. 20734-20750.
51. Liu, C., et al., Preparation of Acid- and Alkali-Modified Biochar for Removal of Methylene Blue Pigment. *ACS Omega*, 2020. 5(48): p. 30906-30922.
52. Kiew, P.L. and J.F. Toong, Screening of Significant Parameters Affecting Zn (II) Adsorption by Chemically Treated Watermelon Rind. *Progress in Energy and Environment*, 2018. 6: p. 19-32.
53. Pande, A., et al., Acid Modified H-USY Zeolite for Efficient Catalytic Transformation of Fructose to 5-Hydroxymethyl Furfural (Biofuel Precursor) in Methyl Isobutyl Ketone–Water Biphasic System. *Energy & Fuels*, 2018. 32(3): p. 3783-3791.
54. Peng, H., et al., Enhanced adsorption of Cu(II) and Cd(II) by phosphoric acid-modified biochars. *Environmental Pollution*, 2017. 229: p. 846-853.
55. Almeida, L.C., et al., Use of conventional or non-conventional treatments of biochar for lipase immobilization. *Process Biochemistry*, 2017. 61: p. 124-129.
56. Lima, J.P., et al. Dehydration of Fructose to 5-Hydroxymethylfurfural: Effects of Acidity and Porosity of Different Catalysts in the Conversion, Selectivity, and Yield. *Chemistry*, 2021. 3, 1189-1202 DOI: 10.3390/chemistry3040087.
57. Chang, C., et al., Study on products characteristics from catalytic fast pyrolysis of biomass based on the effects of modified biochars. *Energy*, 2021. 229: p. 120818.
58. Zeng, H., et al., Efficient adsorption of Cr (VI) from aqueous environments by phosphoric acid activated eucalyptus biochar. *Journal of Cleaner Production*, 2021. 286: p. 124964.
59. Kim, H., et al. Removal Efficiencies of Manganese and Iron Using Pristine and Phosphoric Acid Pre-Treated Biochars Made from Banana Peels. *Water*, 2020. 12, DOI: 10.3390/w12041173.
60. Sonsiam, C., et al., Synthesis of 5-hydroxymethylfurfural (5-HMF) from fructose over cation exchange resin in a continuous flow reactor. *Chemical Engineering and Processing - Process Intensification*, 2019. 138: p. 65-72.
61. Li, Y., et al., A critical review of the production and advanced utilization of biochar via selective pyrolysis of lignocellulosic biomass. *Bioresource Technology*, 2020. 312: p. 123614.
62. Zhang, X., et al., Effects of pyrolysis temperature on biochar's characteristics and speciation and environmental risks of heavy metals in sewage sludge biochars. *Environmental Technology & Innovation*, 2022. 26: p. 102288.

63. Zama, E.F., et al., The role of biochar properties in influencing the sorption and desorption of Pb(II), Cd(II) and As(III) in aqueous solution. *Journal of Cleaner Production*, 2017. 148: p. 127-136.
64. Hoang Phan Quang, H., et al., Nitrate removal from aqueous solution using watermelon rind derived biochar-supported ZrO<sub>2</sub> nanomaterial: Synthesis, characterization, and mechanism. *Arabian Journal of Chemistry*, 2022. 15(10): p. 104106.
65. Wei, Y., et al. Preparation of Porous Carbon Materials as Adsorbent Materials from Phosphorus-Doped Watermelon Rind. *Water*, 2023. 15, DOI: 10.3390/w15132433.
66. Naderi, M., Chapter Fourteen - Surface Area: Brunauer–Emmett–Teller (BET), in *Progress in Filtration and Separation*, S. Tarleton, Editor. 2015, Academic Press: Oxford. p. 585-608.
67. Elnour, A.Y., et al., Effect of Pyrolysis Temperature on Biochar Microstructural Evolution, Physicochemical Characteristics, and Its Influence on Biochar/Polypropylene Composites. *Applied Sciences*, 2019. 9(6): p. 1149.
68. Wang, Z., et al. Characterization of Acid-Aged Biochar and Its Ammonium Adsorption in an Aqueous Solution. *Materials*, 2020. 13, DOI: 10.3390/ma13102270.
69. Özsın, G., et al., A combined phenomenological artificial neural network approach for determination of pyrolysis and combustion kinetics of polyvinyl chloride. *International Journal of Energy Research*, 2022. 46(12): p. 16959-16978.
70. Chen, T., et al., Sorption of tetracycline on H<sub>3</sub>PO<sub>4</sub> modified biochar derived from rice straw and swine manure. *Bioresource Technology*, 2018. 267: p. 431-437.
71. Chu, G., et al., Phosphoric acid pretreatment enhances the specific surface areas of biochars by generation of micropores. *Environmental Pollution*, 2018. 240: p. 1-9.
72. Zeng, X.-Y., et al., Impacts of temperatures and phosphoric-acid modification to the physicochemical properties of biochar for excellent sulfadiazine adsorption. *Biochar*, 2022. 4(1): p. 14.
73. Gong, H., et al., Catalytic conversion of levulinic acid or furfural alcohol into ethyl levulinate using a sulfonic acid-functionalized coffee biochar. *Fuel*, 2023. 352: p. 129059.
74. Bouramdane, Y., et al. Impact of Natural Degradation on the Aged Lignocellulose Fibers of Moroccan Cedar Softwood: Structural Elucidation by Infrared Spectroscopy (ATR-FTIR) and X-ray Diffraction (XRD). *Fermentation*, 2022. 8, DOI: 10.3390/fermentation8120698.
75. Li, H., et al., Biochar derived from watermelon rinds as regenerable adsorbent for efficient removal of thallium(I) from wastewater. *Process Safety and Environmental Protection*, 2019. 127: p. 257-266.
76. Behazin, E., et al., PEER-REVIEWED ARTICLE Mechanical, Chemical, and Physical Properties of Wood and Perennial Grass Biochars for Possible Composite Application. *Bioresources*, 2016. 11: p. 1334-1348.
77. Tong, Y., B.K. Mayer, and P.J. McNamara, Triclosan adsorption using wastewater biosolids-derived biochar. *Environmental Science: Water Research & Technology*, 2016. 2(4): p. 761-768.

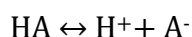
78. El-Nemr, M.A., et al., Amination of biochar surface from watermelon peel for toxic chromium removal enhancement. *Chinese Journal of Chemical Engineering*, 2021. 36: p. 199-222.
79. Chen, J.P. and S. Wu, Acid/Base-treated activated carbons: characterization of functional groups and metal adsorptive properties. *Langmuir*, 2004. 20(6): p. 2233-42.
80. Na, S., et al., Preparation of sulfonated ordered mesoporous carbon catalyst and its catalytic performance for esterification of free fatty acids in waste cooking oils. *RSC Advances*, 2019. 9(28): p. 15941-15948.
81. Puziy, A.M., et al., Phosphorus-containing carbons: Preparation, properties and utilization. *Carbon*, 2020. 157: p. 796-846.
82. Nda-Umar, U.I., et al., Synthesis and characterization of sulfonated carbon catalysts derived from biomass waste and its evaluation in glycerol acetylation. *Biomass Conversion and Biorefinery*, 2022. 12(6): p. 2045-2060.
83. Xu, Z., et al., Mechanistic understanding of humin formation in the conversion of glucose and fructose to 5-hydroxymethylfurfural in [BMIM]Cl ionic liquid. *RSC Advances*, 2020. 10(57): p. 34732-34737.
84. Guo, H., et al., Critical Assessment of Reaction Pathways for Next-Generation Biofuels from Renewable Resources: 5-Ethoxymethylfurfural. *ACS Sustainable Chemistry & Engineering*, 2022. 10(28): p. 9002-9021.
85. Li, M., et al., High conversion of glucose to 5-hydroxymethylfurfural using hydrochloric acid as a catalyst and sodium chloride as a promoter in a water/ $\gamma$ -valerolactone system. *RSC Advances*, 2017. 7(24): p. 14330-14336.
86. Eblagon, K.M., et al., The influence of the surface chemistry of phosphorylated carbon xerogel catalysts on the production of HMF from fructose in water. *Fuel*, 2023. 334: p. 126610.
87. Villa, A., et al., Phosphorylated mesoporous carbon as effective catalyst for the selective fructose dehydration to HMF. *Journal of Energy Chemistry*, 2013. 22(2): p. 305-311.
88. Choi, J., W. Won, and S.C. Capareda, The economical production of functionalized Ashe juniper derived-biochar with high hazardous dye removal efficiency. *Industrial Crops and Products*, 2019. 137: p. 672-680.
89. Deris, N.H., et al. Study the Effect of Various Sulfonation Methods on Catalytic Activity of Carbohydrate-Derived Catalysts for Ester Production. *Catalysts*, 2020. 10, DOI: 10.3390/catal10060638.
90. Shimizu, K.-i., et al., Acidic properties of sulfonic acid-functionalized FSM-16 mesoporous silica and its catalytic efficiency for acetalization of carbonyl compounds. *Journal of Catalysis*, 2005. 231(1): p. 131-138.
91. Combs, E., et al., Influence of alkali and alkaline earth metal salts on glucose conversion to 5-hydroxymethylfurfural in an aqueous system. *Catalysis Communications*, 2013. 30: p. 1-4.
92. Ferreira, K.K., et al., Phosphoric acid-activated carbons as catalysts for 5-hydroxymethylfurfural synthesis. *Biomass Conversion and Biorefinery*, 2023.
93. Zhao, J., et al., Efficient dehydration of fructose to 5-hydroxymethylfurfural over sulfonated carbon sphere solid acid catalysts. *Catalysis Today*, 2016. 264: p. 123-130.

## APPENDIX A

### ACID DISSOCIATIONS

In this section, comparison of type and concentration of acids involved the calculation of basic characteristics related to acid dissociation. Amount of proton ions and anions' functional groups will be calculated using following equation. Notably, acid dissociation constant will be determined at standard temperature of 25°C.

Example of acid dissociation chemical equation:



The equation used to refine concentration of proton ions and anions:

$$K_a = \frac{[\text{H}^+][\text{A}^-]}{[\text{HA}]}$$

Note:  $K_a$  = Acid dissociation constant

$\text{H}^+$  = Concentration of proton ions (M)

$\text{A}^-$  = Concentration of anions (M)

$\text{HA}$  = Initial acid concentration (M)

Table A.1 Comparison of amount of proton ions and anions among various types and concentrations of acids

Samples	Amount of proton and chemical elements per gram of samples (mol/g)			
	Proton ions	Chloride ions	Sulfur groups	phosphorus groups
DWR	-	-	-	-
WB	-	-	-	-
3.2WBC	0.063	0.063	-	-
1.6WBS	0.016	-	0.016	-
3.2WBS	0.032	-	0.032	-
4.8WBS	0.048	-	0.048	-
3.2WBP	0.021	-	-	0.021



## APPENDIX B

### ELEMENTAL COMPOSITIONS

The amount of chemical elements in samples was observed using FESEM/EDX, as displayed in Table B.1. These results supported presence of functional groups reported by FTIR spectra.

Table B.1 Amount of chemical elements in pristine and functionalized biochar

Catalyst	C	N	S	O	P	Cl
WB	56.29	7.65	1.44	26.01	5.54	3.07
1.6WBC	63.61	9.3	0.91	24.57	0.13	1.48
3.2WBC	69.98	7.04	1.53	17.74	0.2	3.5
4.8WBC	64.99	8.26	1.28	20.81	0.12	4.54
1.6WBS	61.93	5.58	3.16	29.15	0.11	0.07
3.2WBS	47.87	9.28	4.04	38.20	0.41	0.2
4.8WBS	60.3	6.78	5.54	27.24	0.07	0.08
1.6WBP	63.85	8.6	0.89	23.43	2.94	0.29
3.2WBP	70.06	6.78	1.26	18.54	3.15	0.21
4.8WBP	65.57	6.54	1.84	20.60	5.37	0.08

## APPENDIX C

### REACTION CONDITIONS

Temperature and time were the main factors in fructose dehydration into 5-HMF. To investigate the remarkable condition of studies catalytic performance in this work. The results on fructose dehydration and 5-HMF yields were shown in Table C.1 and Table C.2, respectively.

Table C.1 Effect of temperature on fructose conversion and product yields (0.2 g catalyst, 40 w/v% fructose, 90 mins)

Temperature (°C)	140	150	160	170	180
Fructose conversion (mol%)	11	41	72	96	100
5-HMF yield (mol%)	7	31	46	49	25
Formic acid yield (mol%)	0	2	5	13	18
Levulinic acid yield (mol%)	0	2	5	14	31
Furfural yield (mol%)	0	1	1	2	2
Other products such as humin, unknown (mol%)	92	64	43	23	23
5-HMF selectivity (%)	68	78	63	51	25

Table C.2 Effect of time on fructose conversion and product yields (0.2 g catalyst, 40 w/v% fructose, 160°C)

Time (mins)	60	90	120	150
Fructose conversion (mol%)	61	72	85	92
5-HMF yield (mol%)	38	46	47	45
Formic acid yield (mol%)	4	5	8	11
Levulinic acid yield (mol%)	3	5	8	13
Furfural yield (mol%)	1	1	1	1
Other products such as humin, unknown (mol%)	54	43	36	40
5-HMF selectivity (%)	63	63	55	48

## VITA

**NAME** Pimlapas Bunwichian

**DATE OF BIRTH** 20 January 1999

**PLACE OF BIRTH** Chonburi

**INSTITUTIONS ATTENDED** Chulalongkorn university

**HOME ADDRESS** 188/120 Piyawat village M.3 Samet Mueang Chonburi 20000

**PUBLICATION**

1. Pimlapas Bunwichian, Giang T. T. Le, Sanchai Kuboon, and Tawatchai Charinpanitkul, "Transformation of watermelon rind to functionalized biochar for catalytic conversion of fructose to 5-HMF", Proceeding of 11th Joint Conference on Renewable Energy and Nanotechnology (JCREN2023), Davao City, Philippines, January 20-21th, 2023
2. Pimlapas Bunwichian, Sanchai Kuboon, and Tawatchai Charinpanitkul, "Effect of sulfonic group on characteristics and performance of sulfonated biochar catalyst for fructose dehydration to 5-HMF", Proceeding of Silpakorn International Conference on Total Art&Science (SICTAS2023), Phetchaburi, Thailand, November 8-10th, 2023